NATIONAL AERONAUTICS AND SPACE ADMINISTRATION

Technical Memorandum 33-806

Absolute Flux Density Calibrations of Radio Sources: 2.3 GHz

JET PROPULSION LABORATORY
CALIFORNIA INSTITUTE OF TECHNOLOGY
PASADENA, CALIFORNIA

December 1, 1977

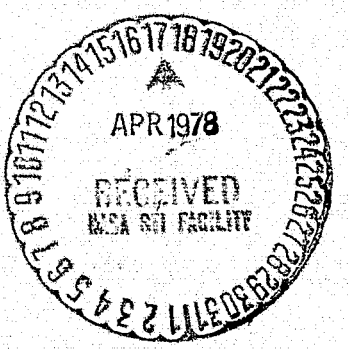

NATIONAL AERONAUTICS AND SPACE ADMINISTRATION

Technical Memorandum 33-806

Absolute Flux Density Calibrations of Radio Sources: 2.3 GHz

A. J. Freiley, P. D. Batelaan,
and D. A. Bathker

JET PROPULSION LABORATORY
CALIFORNIA INSTITUTE OF TECHNOLOGY
PASADENA, CALIFORNIA

December 1, 1977

PREFACE

The work described in this report was performed by the Telecommunications Science and Engineering Division of the Jet Propulsion Laboratory.

ACKNOWLEDGMENTS

The authors wish to thank Dr. M. J. Klein, Dr. C. T. Stelzried, and G. S. Levy of JPL for their helpful discussions and advice that contributed greatly to the results of this program and to the operations personnel of the Venus Station at Goldstone, California for their diligence during the observing sessions. Appreciation is also extended to H. Reilly, R. Thomas, R. Gardner, J. Withington, O. Hester, and M. Garland of JPL for their technical assistance to the program. The fundamental contributions by the National Bureau of Standards, Boulder, Colorado, are acknowledged and detailed within.

ABSTRACT

This report is a detailed description of a NASA/JPL Deep Space Network program to improve S-band (2.3 GHz) gain calibrations of large aperture antennas. The program is considered unique in at least three ways; first, absolute gain calibrations of high quality suppressed-sidelobe dual mode horns first provide a high accuracy ($\pm$0.04 dB or better than $\pm$1 percent with 3σ confidence) foundation to the program. Second, a very careful transfer calibration technique using an artificial far-field coherent-wave source was used to accurately ($\pm$0.21 dB or better than $\pm$5% with 3σ confidence) obtain the gain of one large (26 m) aperture. Third, using the calibrated large aperture directly, the absolute flux density of five selected galactic and extragalactic natural radio sources was determined with an absolute accuracy better than 2 percent, now quoted at the familiar 1σ confidence level. The follow-on considerations to apply these results to an operational network of ground antennas are discussed. It is concluded that absolute gain accuracies within $\pm$0.30 to 0.40 dB (with 3σ confidence) are possible, depending primarily on the repeatability (scatter) in the field data from Deep Space Network user stations.

This report should be of considerable interest to a wide audience; those concerned with electromagnetic standards, antenna and microwave engineers, radio astronomers, and finally those responsible for carefully evaluating, operating and maintaining ground facilities of a similar kind.

CONTENTS

Tables

SECTION I

INTRODUCTION

The NASA/JPL Deep Space Network (DSN) is one link of an overall telecommunication system that collects, transmits, and receives information between deep space probes and Earth and incorporates three major complexes which are strategically located at widely separated Earth locations (California, Australia, and Spain) to provide 24-h per day coverage for deep space probe communications and radio science observations. Each DSN complex has several large ground-based reflector antennas with associated station facilities. Each complex in Spain and Australia has one 64-m and two 26-m diameter antennas and the California Deep Space Communications Complex has one 64-m and three 26-m antennas.

Utilization of a large ground-based antenna for spacecraft communications or for absolute flux measurements in radio or radar astronomy requires accurate knowledge of the antenna gain and related aperture efficiency. When used as a radio telescope for absolute flux measurements, errors due to inadequate knowledge of the antenna gain give rise to directly corresponding errors in the flux measurement. In contrast, the uncertainties arising from poorly known antenna gain for the spacecraft communications service are more subtle, and frequently have a major impact. Spacecraft mission design, especially important telemetry data rate selections that frequently determine data volume returned, as well as operations planning and execution, are all dependent upon accurate knowledge of the ground antenna gain, in some instances critically so (tenths of a dB). When ground facilities are viewed in the additional light of reuseability (applicability to more than one spacecraft mission), it is not difficult to appreciate the probable cost effectiveness of very accurate calibrations of the ground antenna gain, compared with available alternatives of improving the overall link performance specification in some other way (bigger spacecraft antenna, lower noise ground receiver, and others). A side benefit of such improved calibrations accrue to related activities; basic radio and radar science objectives, for example. Accordingly, an Antenna Gain Calibration Program (AGCP) was undertaken by JPL to achieve operational S-band ground antenna gain absolute accuracies within ± 0.30 to 0.40 dB, with very high confidence (3σ).[1] Initial engineering estimates indicated that an achievable overall project accuracy of ± 0.25 dB should be possible. Final program results indicate that operational stations can be gain calibrated from ± 0.23 to ± 0.37 dB, depending primarily on the quality (repeatability) of the field data returned from user stations.

---

[1]Unless otherwise specified, uncertainties quoted throughout this report are to be interpreted as very high confidence; either equal to or, in essence, $\pm 3\sigma$. All uncertainties are treated as gaussian to simplify the error analysis even though some uncertainties may not be so distributed.

The AGCP was designed and divided into four major parts: a fundamental portion stressing fieldworthy antenna gain and microwave attenuator (working) standards, a part stressing the far-field and coherent wave calibration of a single large aperture (master) ground station, a portion to determine absolute flux from selected galactic and extragalactic natural radio sources using the calibrated master aperture, and the final part dealing with use of the then-calibrated natural sources by large aperture user stations. In the program, the high flux level galactic source (Cassiopeia A) was included primarily for intercomparisons with absolute flux scales determined elsewhere with other calibration techniques; several intermediate flux level extragalactic sources were included primarily for purposes of this program and, in valuable related work by Klein and Stelzreid (Ref. 1-1) using the same large master antenna, a number of low-flux level point sources were examined on a high precision (ratio) basis, and can now be tied into the absolute flux scale.

Figure 1-1 gives an overview of the entire program. Five JPL developed suppressed sidelobe dual mode horns were calibrated, both at JPL in Pasadena, California, and at NBS in Boulder, Colorado. Available X-band scale models were used to initiate the program in a timely manner. Later, three S-band horns were used; two undergoing various range calibrations while an "identical" third working unit was used at the master 26-m station to initiate that program phase in a timely manner. Later, the working field standard underwent most careful post calibrations. This work established the simple sum uncertainty of all gain standard horn error sources as within ± 0.04 dB for the calibration standards and ± 0.06 dB for the working standard (in situ). The master 26-m station, in turn, was calibrated using narrowband technique to ± 0.21 dB, with very high confidence. The narrowband (CW) technique was made possible when the Apollo Lunar Surface Experiment Package (ALSEP) was placed in unattended operation on the Moon by the Apollo astronauts. ALSEP offered a true far-field point source CW signal, well suited to large antenna gain measurements. The primary error sources involved in that step were the working standard horn (± 0.06 dB), the working attenuator standard (± 0.06 dB) and the repeatability of the low-level measurements (± 0.18 dB). Next, the selected natural radio sources were calibrated using the master station.[2] That work is carefully analyzed to show the sources are calibrated from ± 0.22 to 0.25 dB (3σ), or better than ± 2 percent, quoted on the familiar 1σ basis.

Finally, limited experience in data collection from the follow-on user stations tracking the previously calibrated sources, shows an absolute accuracy of ± 0.23 dB is the best achievable. Depending on repeatability of the measurements, the accuracy is not expected to degrade beyond ± 0.37 dB, for relatively scattered data. The program thus meets the initial goal of ± 0.30 to ± 0.40 dB for an operational network of ground

---

[2]In practice, gain comparison measurements and natural source measurements were interlaced in time, to avoid questions of antenna gain deterioration with time, configuration changes, etc.

antennas, which are not particularly instrumented for true radioastronomical work (use of non-gain-stabilized total power radiometers, for example). Accurately, well-calibrated horn antennas for a variety of other radiometric activities and a well-calibrated master station providing a variety of other uses are two indirect benefits of the program.

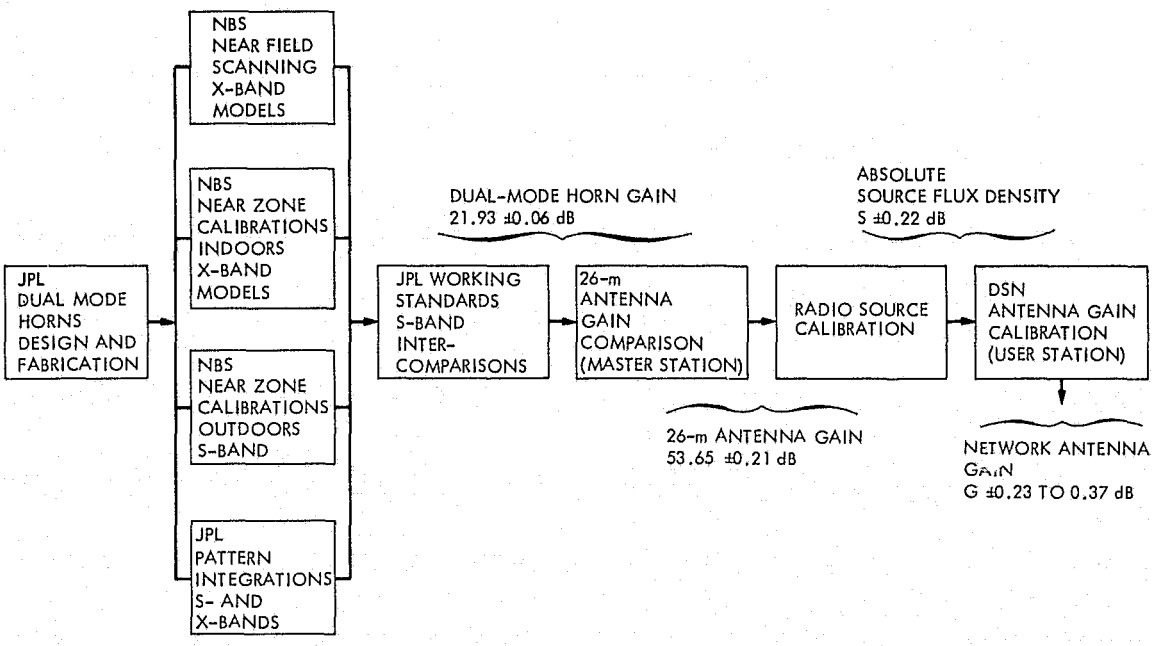

Fig. 1-1. Antenna Gain Calibration Program Summary

SECTION II

GAIN STANDARD HORN CALIBRATION

A. Horn Selection

In this section, the selection and precision calibration of the gain standard horns used in the JPL AGCP are discussed. Potter (Ref. 2-1) first described the superposition of the TE_{11} and TM_{11} waveguide modes in a smooth wall conical horn of small flare angle, and about 5λ aperture, initially for use as a feedhorn for Cassegrain antennas. It has long been recognized that the advantages of such a horn--equal beamwidths in all planes, complete phase center coincidence, suppressed sidelobes and polarization independence--make it an ideal candidate for gain standard applications. By 1970, considerable experience had accumulated at JPL by Ludwig and others (Ref. 2-2) in successfully reproducing the measured radiation patterns of such horns by an analysis including the above-mentioned modes and a small TE_{21} component. Figure 2-1 shows the remarkable results of a comparison of analytical work and precision measured radiation patterns of a JPL dual mode horn for both principal- and cross-polarization components in the diagonal planes of the horn (ϕ = 45 deg). Essentially identical agreement was obtained in the E- and H-planes; of course, theoretically, no cross-polarization components exist in those planes. Because of the demonstrated close agreement between theoretical and experimental radiation patterns, coupled with the ability to obtain the pattern directivity, a high confidence was developed in the application of dual mode horns as gain standards. This confidence is further supported by the superior pattern sidelobe performance. That is, in real-world applications, a dual mode horn is less likely to contribute to system errors due to wide-angle multipath. Further, JPL work with the spherical wave expansion technique was perfected, giving support to the necessary near-zone and/or even possible near-field gain measurements. This technique allows a finite range experimental radiation pattern to be extended analytically forward to an infinite range pattern (or conversely, an infinite range theoretical radiation pattern back to a finite range pattern) (Refs. 2-3 to 2-5). Some initial horn gain measurements by conventional range and pattern integration techniques are available (Refs. 2-6 to 2-8). Substantial evaluation and application of horns essentially identical to those used in this program proceeded at JPL through the middle and late 1960's (Refs. 2-9 to 2-12).

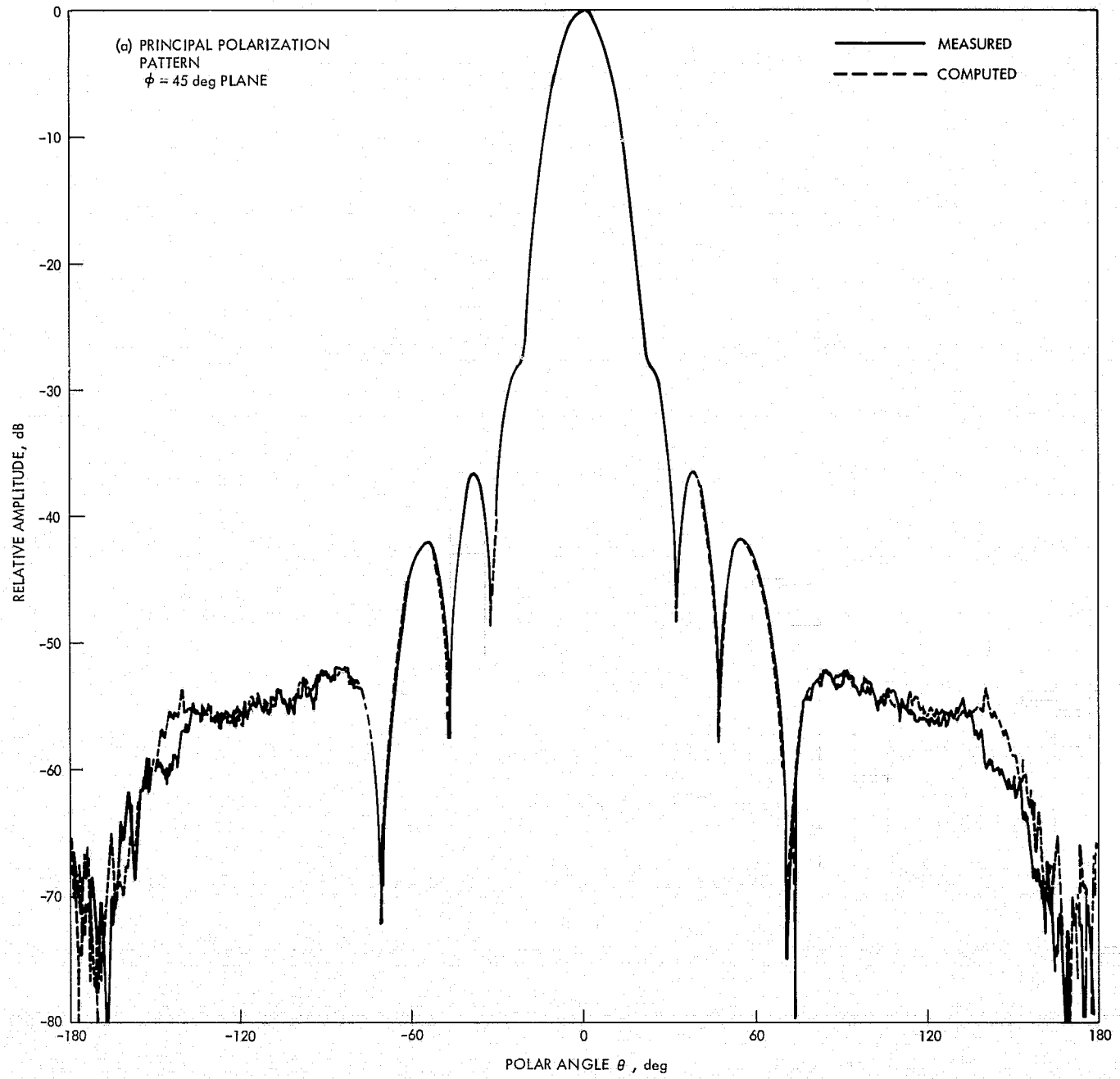

Fig. 2-1a. Computed and Measured Horn Patterns for Principal Polarization

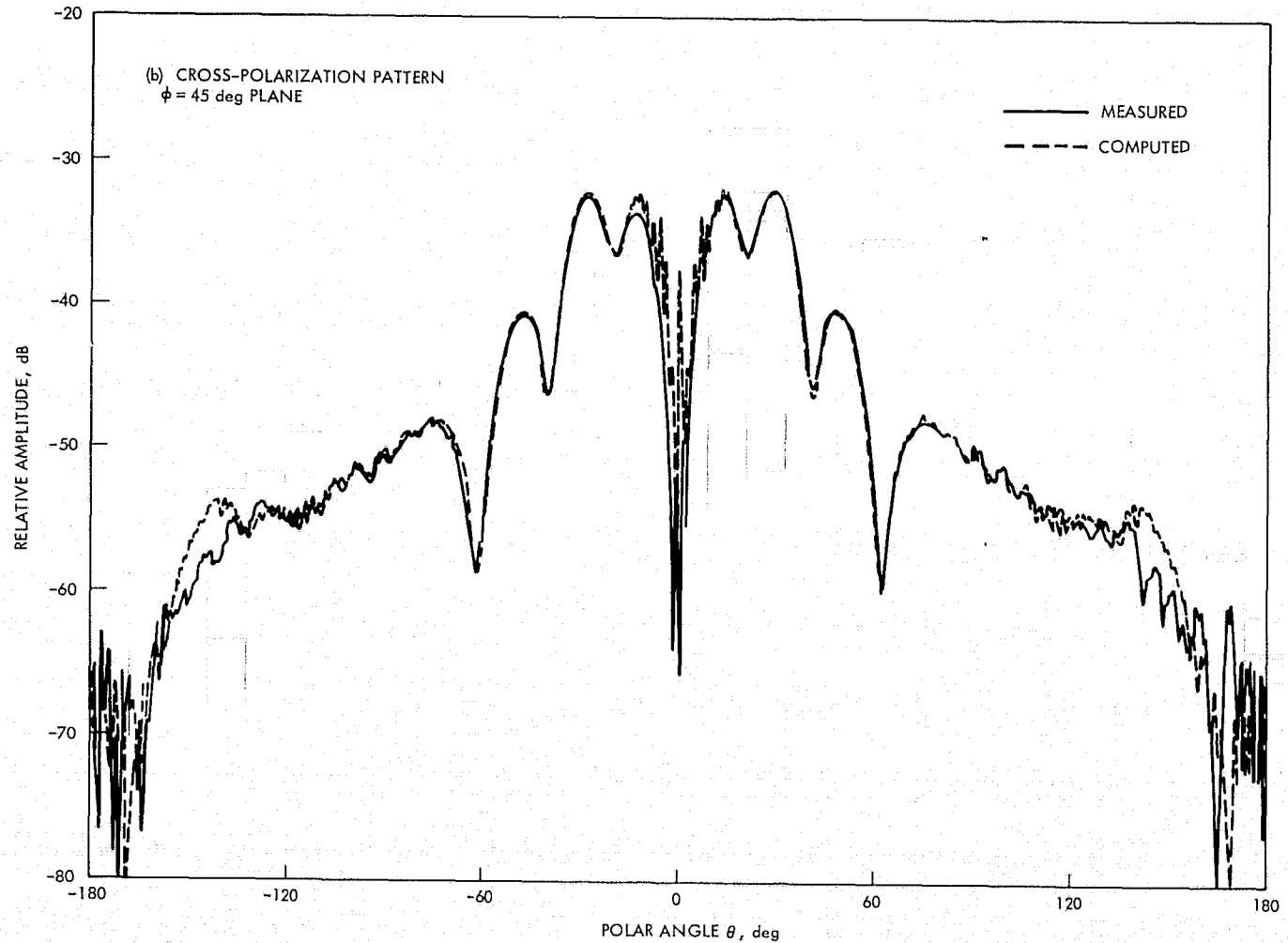

Figure 2-1b. Computed and Measured Horn Patterns for Cross Polarization

B. Absolute Gain Calibrations

1. Techniques

A cooperative effort between the Jet Propulsion Laboratory (JPL) and the National Bureau of Standards (NBS) resulted in the gain measurement of five nominally identical dual mode horn antennas--two X-band and three S-band models--using three independent techniques: (1) a near-field scanning method; (2) the near zone (extrapolation) method, and (3) the pattern integration method. The planar near-field scanning method applied by NBS was used to measure the X-band scale model horns with high accuracy, primarily limited only by the few restrictive approximations necessary in this technique. From the near-field scans the far-field radiation patterns and gain can be determined quantitatively (Refs. 2-13 and 2-14). The near zone (extrapolation) technique was also applied by NBS to determine the power gain of the horns. This technique is based on a generalized two-antenna approach at reduced range distances and measures absolute gain including corrections for errors due to proximity and possible multipath effects (Refs. 2-13 and 2-14). The pattern integration method applied by JPL involves a spherical wave expansion of the horn radiation pattern from a finite experimental range to an infinite range. The JPL pattern integration measurements were conducted on the scaled X-band horns with excellent results (Ref. 2-3), and the agreement with the NBS measurements is very good. The total independence of the above three evaluation methods should be noted.

2. Results

The measurements of the dual-mode horns agree extremely well among the three calibration techniques. The gain results reported by NBS in Appendix A were measured at six different frequencies in the operating band of the horns for both linear polarization and right-hand-circular polarization. The gains for linear polarization at 2295 MHz are 22.029 dB for Horn I (G_1) and 22.078 dB for Horn II (G_2) where the high confidence ± 0.036 dB uncertainties are estimated and handled conservatively as simple sums. The results of the pattern integration work measured directivities of the linearly polarized X-band scaled models at 8448 MHz (2295 MHz scale) as 22.03 dB and 22.05 dB, with a high confidence estimated uncertainty of ± 0.10 dB (Ref. 2-3).3

3An analysis of the expected dissipation loss of the dual mode horns indicates about 0.005 dB at S-band and 0.020 dB at X-band. Here, we compare the S-band power gains (directivity reduced by dissipation) loosely with the X-band directivities obtained from pattern integration, simply to quickly show the general tenor of favorable agreement seen throughout this phase of the program.

The circular polarized horn gain measurements over a 20-MHz frequency band are plotted and fit in Fig. 2-2 making possible a simple curve fit interpolation to 2278.5 MHz, the frequency at which the coherent-wave large aperture antenna gain calibration was to be performed in a later program phase. The gains of the horns were determined to be 21.945 dB and 21.963 dB for Horns I and II, respectively, with a conservative simple sum uncertainty of ±0.036 dB. At the time of this writing, the complete report on gain calibrations by NBS and the detailed error analysis have not been fully documented, but may be available at a later date. In the interim, Appendix A gives the succinct and important results of their work at S-band. It should be noted that although, in principle, the three independent horn measurement results could be combined to obtain a fully defensible higher accuracy result, it was deemed advisable to remain at the approximate ±0.04 dB level. A part of this decision is based on the preliminary NBS results and the magnitudes of other error sources will be seen to dominate the final results of our overall program.

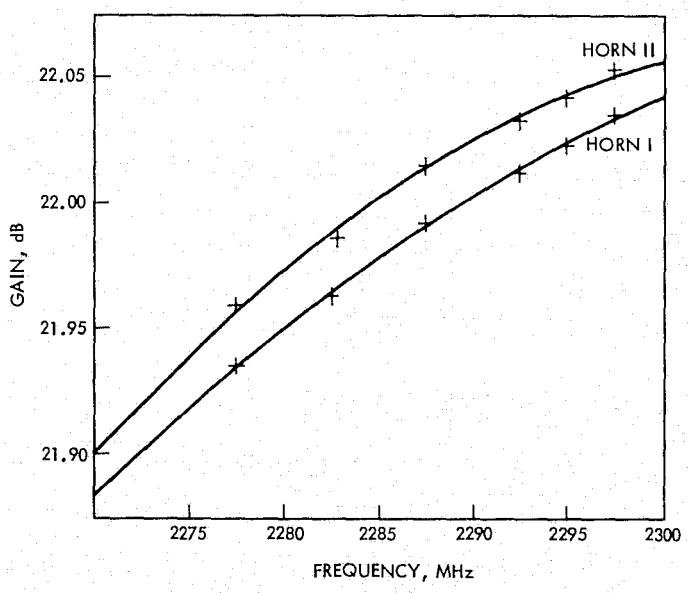

Fig. 2-2. JPL/NBS Horn Antenna Gain Calibration as a Function of Frequency

C. Working Horn Comparison

In order to initiate the program and efficiently utilize schedule time on the 26-m diameter master antenna located at the (Venus) Deep Space Station (DSS-13),[4] a third S-band gain standard horn antenna was fabricated to the same mechanical tolerances as the original horn antennas being calibrated by NBS. The third horn became the working field standard (designated the Venus horn) and was the actual unit installed on the master 26-m antenna. This allowed the NBS standards work and the JPL station calibration work to proceed in parallel.

After completion of the master station calibration and the NBS horn calibrations, the Venus horn was dismounted from the 26-m antenna. A very careful gain comparison measurement was conducted among the NBS calibrated gain standard horns and the Venus horn. The objective of the gain comparison measurement was to determine the absolute gain of the Venus horn and the associated uncertainty. The gain calibration of the Venus horn was determined at two frequencies: the prime frequency of 2278.5 MHz was measured to complete the gain determination of the far-field coherent wave portion of the program, and the secondary frequency of 2295 MHz was measured to anticipate future needs for the Venus horn as a working gain standard horn, at the DSN midband frequency.

1. Antenna Range Evaluation

The antenna range used to calibrate the Venus horn is part of the JPL Mesa Antenna Range facility. Figure 2-3 shows this range with the gain standard horns mounted in a typical measurement configuration. The two horns on the left, in positions I and II were under test, and the third horn on the right in position III was the illuminator. The power output level of the two horns under test was compared and the differential gain was determined by alternately switching between the two horns. The block diagram of the measurement system used to perform the horn comparison is given in Fig. 2-4.

The S-band signal source was frequency stabilized and amplitude leveled to insure system stability. In addition, the test and reference signals were differenced to further stabilize drift and instabilities of the system. The signal level was recorded as analog and digital data for processing. The level set variable attenuator provided a convenient method to verify the gain response of the detectors. By varying the signal level at this point in the system both the reference and the test signals should respond in the same manner; therefore, the difference between the two should remain constant. To insure an acceptable response both detectors were operated at about the same power level. Over a 0.5-dB level change of the level set variable attenuator the normalized output response of the sensitive recording system varied no more than 0.001 dB. The gain difference between horns was expected to be in the

[4]Goldstone, California, USA.

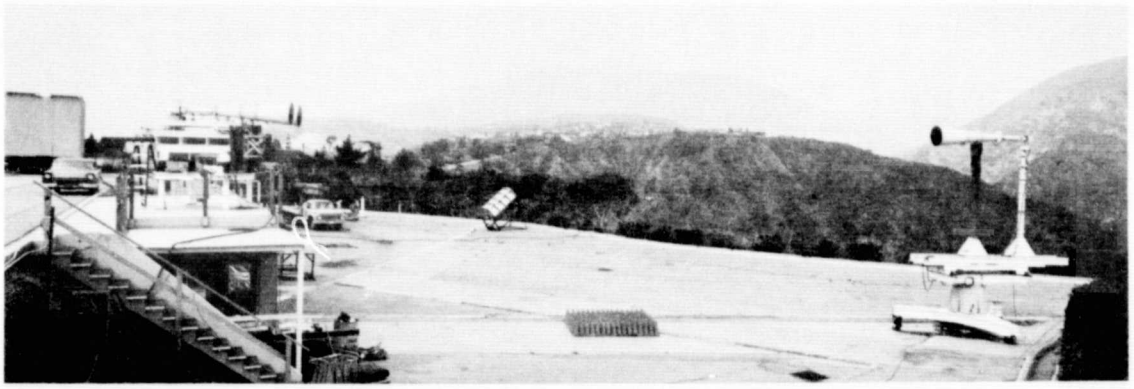

Fig. 2-3. JPL Antenna Range Used in Horn Comparisons

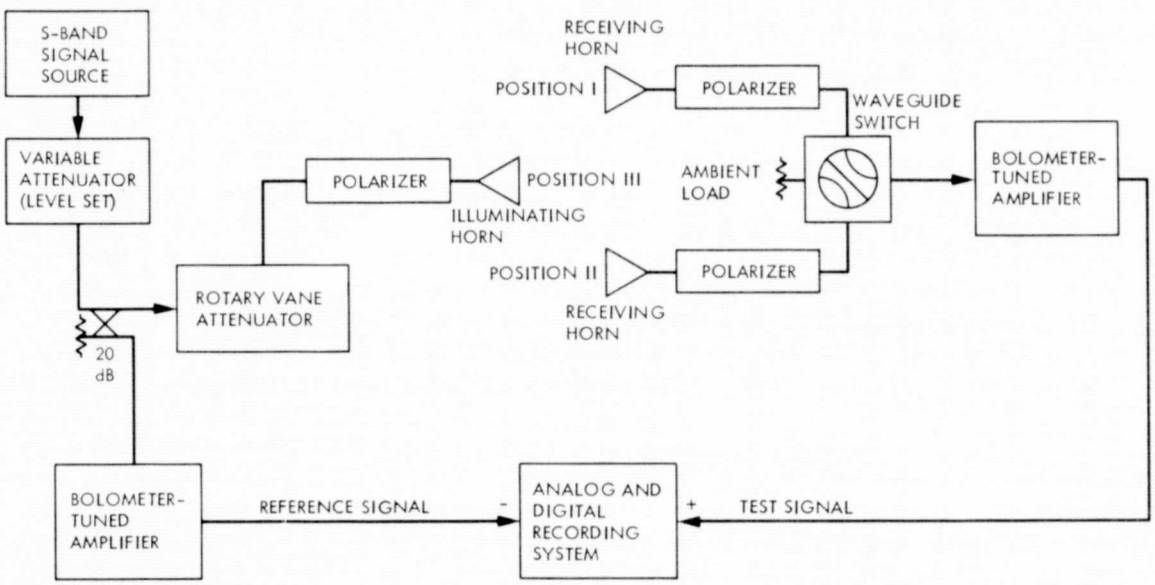

Fig. 2-4. Horn Gain Comparison Measurement System Block Diagram

range of 0.05-dB. If detector responses are assumed to be linear, the error due to the gain response of the detectors would be about ± 0.0003 dB (3σ).

The horns achieve circular polarization by injecting a linearly polarized signal into a quarter wave plate polarizer which produces right-hand circular polarization with an on-axis ellipticity of less than 0.2 dB. To reduce the small polarization loss between illuminator and receiver horns, the two horns were positioned to have good alignment of the slightly elliptical polarization. This alignment was measured to be within 2 deg (rotationally). With two horns each exhibiting ellipticity of 0.2 dB and aligned with 2 deg, the polarization loss contributed less than ± 0.0015 dB (3σ) error to the measurement.

The receiving system consisted of two horn antennas and their associated polarizers connected to a waveguide switch that alternately switched the bolometer detector between the two horns. To minimize the differential waveguide loss between the two horn positions, the switch was operated in such a way as to utilize the same path through the rotor of the switch. The differential waveguide loss between the output port of each horn and the detector port was measured to be less than ± 0.0018 dB (3σ).

During the horn comparison measurements, the horns under test were moved alternately on boresight of the illuminator horn as shown in Fig. 2-5. The optical alignment between the illuminator and the test horns was sighted as repeatable within 0.02 deg. Assuming a gaussian beam shape with a 15-deg halfpower beamwidth and the stated misalignment, the gain loss resulted in a negligible error. Throughout the gain comparison measurements the horn mounted on the rotator was used as the illuminator, necessitating no position change; therefore, the accuracy of the angle readouts contributed no errors to the measurement.

Range interference generally poses a difficult problem, but by the very nature of this gain comparison measurement, many effects canceled or became less significant due to the fact that most effects were more-or-less equally received by both horns. The reflection and ground-bounce multipath were experimentally determined by varying the spacing between the illuminator and receiver horns. The initial measurements of multipath indicated the usual linear downward slope of the signal envelope due to inverse square "space loss" increase and a 0.3-dB peak-to-peak ripple. When the illuminator and receiver masts and mid-zone between the horns were covered with RF absorber the ripple of the multipath was reduced to about 0.03 dB peak to peak. The gain comparison measurements were then performed at three range spacings to experimentally examine the effect of this residual multipath. The three range spacings corresponded to the maximum, minimum, and middle of the ripple pattern. The data indicated no measurable effect in the differential gain of the horns due to the three spacing positions. Two other sources of interference, the radiation leakage into the cables and the system leakage between generator and receiver directly were also experimentally examined by terminating the receiver detector into a load and comparing the difference between horn positions I and II. With careful assembly and the use of aluminum tape as RF shielding, the

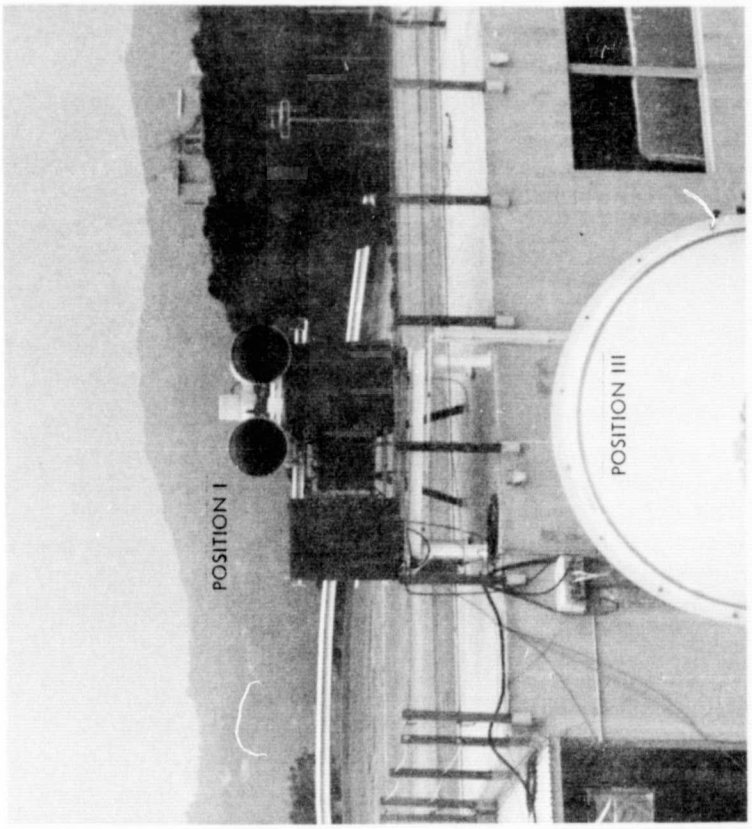

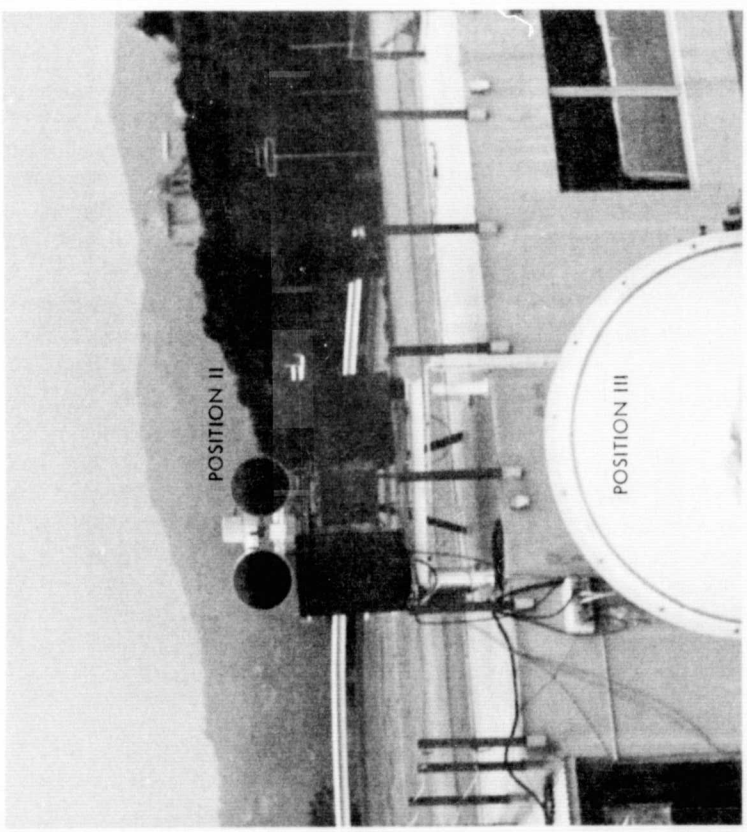

Fig. 2-5. Horn Positions for Gain Comparison Measurement

interference between the two horn positions was below the sensitivity of the receiving system resulting in no measurable effect.

To investigate the effect of the two horns in position I and II in near proximity to one another (side by side), a device termed a hat was constructed. The hat consisted of RF absorber in a configuration which covered the aperture and the first 20 cm of the horn's exterior. Gain comparison measurements were performed both with and without the hat on the unused horn and the results indicated no measurable difference. Therefore, the effect of the two horns in near proximity to one another was not considered to be a problem.

The receiver and data recording system were calibrated by stepping a highly accurate rotary-vane attenuator in precise steps through the expected operating range. A sample of an analog recording of a calibration is given in the lower portion of Fig. 2-6. The overall calibration error based on the used portion of the rotary-vane attenuator is ± 0.003 dB (3σ) (Ref. 2-15). The calibration checks between gain measurements were repeated at regular intervals. The system calibration remained constant throughout the duration of the horn calibration measurements.

2. Horn Gain Comparison Results

To complete the gain comparison measurements each pair combination of the three S-band horns was tested. The comparison of each pair of horns was the result of some 36 measurements. Each gain comparison measurement was accomplished by establishing a receiver level on the reference horn, then by rotating the waveguide switch to the test horn and sliding the test horn sideways onto boresight, a receiver level was established for the test horn. To account for any drift over the measurement time period, the reference receiver level was reestablished by returning the slide to the reference horn position. The two reference horn receiver levels were averaged and compared to the test horn receiver level to determine the differential gain between the reference and test horns. The analog recording of one measurement of the gain difference between Horn II and the Venus horn is given in the upper portion of Fig. 2-6. In order to experimentally determine any asymmetry between horn positions I and II, the test and reference horns were interchanged and the gain comparison measurements were repeated. The measurement indicated no measureable differences due to horn positions.

The differential gain determination at 2278.5 MHz indicated the horn identified as Horn II has the highest gain followed by Horn I and Venus horns in order of decreasing absolute gain. The gain difference between the Horn I and Horn II was measured to be 0.029 dB. The gain relationship is given as

$$G_{II} = G_I + 0.029 \text{ dB}$$

where G is the gain of the indicated horn in dB. The NBS absolute gain measurement indicates a gain difference of 0.022 dB, which agrees very well within the uncertainty of both sets of measurements. The gain difference

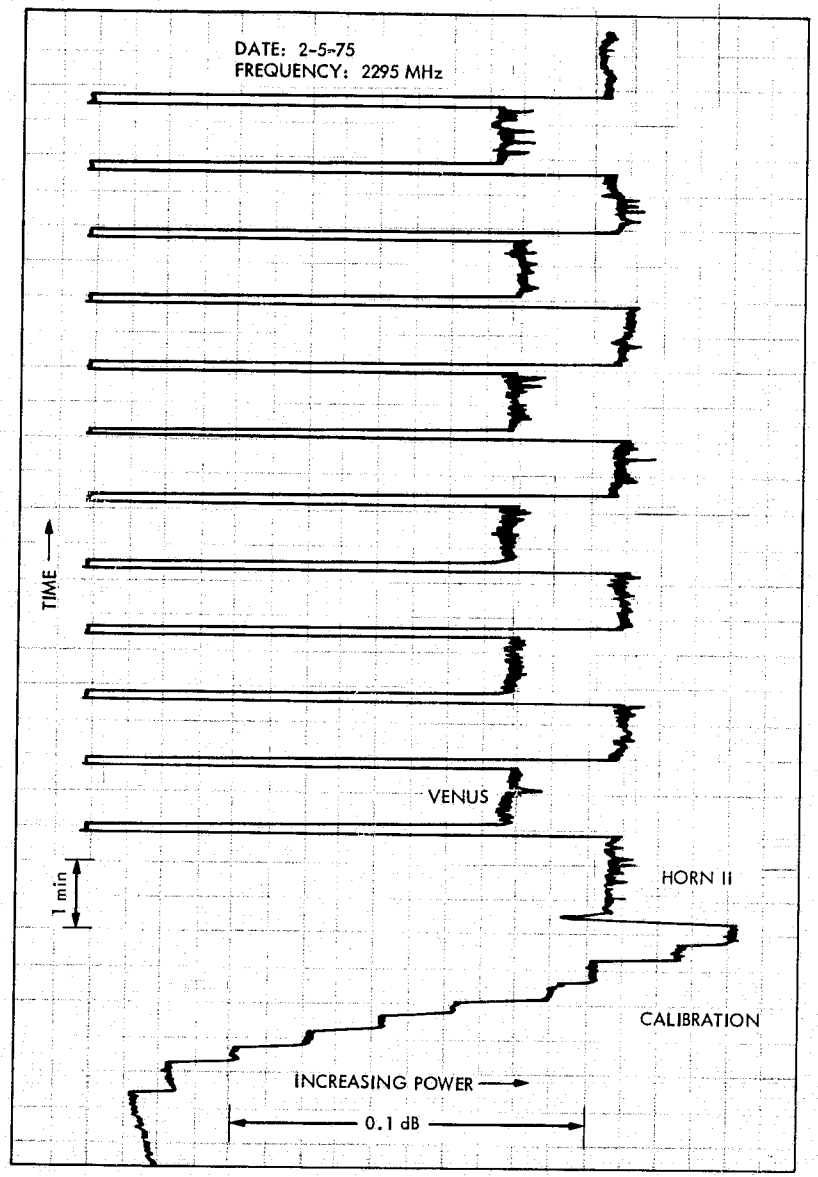

Fig. 2-6. Sample Analog Recording of System Calibration and Gain Comparison

between Horn I and the Venus horn was measured to be 0.011 dB and is given as

$$G_I = G_{Venus} + 0.011 \text{ dB}$$

To complete the series of the measurements, the gain difference between Horn II and the Venus horn was (redundantly) measured to be 0.043 dB and is given as

$$G_{II} = G_{Venus} + 0.043 \text{ dB}$$

Within this set of measurements the gain difference between Horn II and Venus horns should be the sum of the other two difference measurements (i.e., 0.029 + 0.011 = 0.040 dB). Therefore the difference expected was 0.040 dB but the measured value was 0.043, which is excellent agreement, considering the uncertainties of this measurement technique.

At 2295 MHz[5] the differential gain determination indicates the same order of difference as at the lower frequency. From highest to lowest gain the order remains: Horn II, Horn I, and Venus horns. The gain difference between Horns I and II was measured to be 0.025 dB and is given as

$$G_{II} = G_I + 0.025 \text{ dB}$$

The NBS results indicate a gain difference at 2295 MHz of 0.019 dB, which again agrees well within the uncertainty of both measurements. The gain difference between I and the Venus horns was measured to be 0.013 dB and is given as

$$G_I = G_{Venus} + 0.013 \text{ dB}$$

The gain difference between Horn II and the VENUS horn was finally (redundantly) measured to be 0.030 dB and is given as

$$G_{II} = G_{Venus} + 0.030 \text{ dB}$$

Considering this set of measurements, the gain difference between Horn II and the Venus horn should have been 0.038 (i.e., 0.025 + 0.013) but was somewhat less. To within the uncertainties of the measurement the gain differences measured are entirely reasonable. The dominant error source is the measurement scatter, as can be seen in Table 2-1.

5As stated, 2295 MHz tests were done primarily to anticipate future needs for the Venus horn at the DSN midband frequency. Actually, for purposes of this Section, the work is viewed as further examining and substantiating the claimed precisions (different multipath situation, for example).

Table 2-1. Gain Uncertainty Due to Horn Gain Comparison Measurements

Source of uncertainty	Uncertainty dB, 3
Differential detector response	±0.0003
Polarization loss	≤ ±0.0015
Differential waveguide loss	≤ ±0.0018
Alignment between horns	Negligible
Range interference	Negligible
Horn interaction	Negligible
Rotary-vane attenuator calibration (over the range used)	±0.003
Measurement scatter	±0.018
Simple sum	±0.025

D. Absolute Horn Gain Summary

The gain characteristics of the conical dual-made horn antennas have been determined independently by JPL and NBS using several techniques for linear polarization. The NBS measurements indicate gains of 22.029 and 22.078 dB with a simple sum uncertainty of ±0.036 dB at 2295 MHz. The pattern integration technique, applied to the X-band scale models by JPL, indicated expected S-band gains of 22.03 and 22.05 dB for X-band JPL horns 1 and 2, with a 3σ uncertainty of ±0.10 dB. The excellent agreements in the gain of the horn antennas generated a high level of confidence in the results of each technique.

The absolute gain determination of the circular polarized working gain standard (Venus) horn is based on near-zone horn measurements reported by NBS at 2277.5 and 2282.5 MHz, interpolated at 2278.5 MHz. Based on the calibration of Horns I and II interpolated at 2278.5 MHz, the gain of the Venus horn is 21.930 and 21.920 dB, respectively, yielding

a mean gain value of 21.925 dB. By a similar deduction the gain of the working standard at 2295 MHz is determined to be 22.011 db.[6]

The uncertainty associated with the gain of the working standard gain horn is the accumulation of the uncertainties of the NBS calibration and the JPL gain comparison. The uncertainty of the near zone measurements performed by NBS, considered to be very conservative, was estimated to be ±0.036 dB, simple sum, for the worst case condition. The errors of the near zone measurement might be considered independent (the RSS uncertainties would be about ±0.015 dB) but insufficient time has been devoted to this level of accuracy determination.[7] To maintain the consistency of the horn calibration accuracies then, the uncertainty of the horn comparison measurement is also specified as a simple sum (±0.025 dB). Then, the simple sum uncertainty of the working gain standard horn is very conservatively taken as the sum of simple sums (±0.061 dB), with high confidence. The absolute gains of the calibrated horns are summarized in Table 2-2. The calibration of the working standard is well understood and is traceable to NBS standards.

---

[6]It is interesting to note the "identical" five horns yield rounded value linear polarization gains of 22.01, 22.03, 22.03, 22.05 and 22.08 dB, at (or scaled to) 2295 MHz. The simple average value gain is 22.04 dB; the same value holds considering either pattern integration or range extrapolation techniques.

[7]Presumably a careful evaluation of the errors in the NBS near zone measurement would result in an overall accuracy of ±0.015 to ±0.036 dB. Since the higher value was well within the initial program goals for that phase of the work (which was ±0.050 dB), the full evaluation has been deferred. The most careful work by NBS in this connection deserves recognition.

Table 2-2. Absolute Gain of Standard Horns With Associated Uncertainty

Horn	Absolute gain, dBi			Comments
	2278.5 MHz circular polarized[1]	2295.0 MHz circular polarized[1]	8848 MHz linear polarized[2,3,4] (X-Band Model)	
JPL/NBS I	21.941±0.036	22.023±0.036	---	NBS near zone calibration
JPL/NBS II	21.963±0.036	22.042±0.036	---	NBS near zone calibration
Venus	21.925±0.061	22.011±0.061	---	JPL gain comparison
JPL 1	---	---	22.05±0.10	JPL pattern integration
JPL 2	---	---	22.03±0.10	JPL pattern integration

[1]Simple sum uncertainty.

[2]Root-sum squared uncertainty

[3]The model scales to 2295.0 MHz.

[4]As discussed, the X-band values are directivities. Absolute gains are reduced approximately 0.02 dB due to dissipation. Directivities are shown for comparison with S-band, where dissipation approaches a negligible value.

SECTION III

MASTER STATION CALIBRATION

A. Introduction

Several areas of concern existed in the gain transfer calibration of the gain standard horn to the master 26-m aperture. From the hardware point of view, physical placement of the gain standard horn was perhaps most important, followed by concern for a fieldworthy S-band variable attenuator. In the operations context, the sequence of obtaining and recording data was very important. Weak (-160 dBmW) signals were available on the gain standard horn, and modest (-129 dBmW) levels were present at the output of the large aperture using the narrowband RF carrier of the selected lunar ALSEP signal source. In both cases the signals had to be carefully tracked in position (antenna pointing) and in frequency, to utilize a narrow receiver noise bandwidth.

B. Technique

The technique for measuring the master antenna gain was a variation of the conventional gain comparison method. In the gain comparison method, a far-field beacon is sequentially observed by a standard gain horn of known power gain, and then by the large antenna to be measured. In addition, the two antennas also view the background space by sequentially pointing off-source. The four observations -- on-source/off-source for the standard antenna, and on-source/off-source for the large antenna -- can then be used to solve for the power gain of the large antenna (Ref. 3-1). Instead of pointing off-source physically with the standard and large antennas, the variation used here was to tune off the narrow-band CW signal source with the phase-lock receiver. In reality the receiver (refer to block diagram, Fig. 3-1) was tuned off the far-field beacon and tuned to receive a test signal which was injected locally in front of the maser preamplifier. A precision attenuator was first used to adjust the amplitude of the test signal level to match the far-field beacon signal amplitude received by the standard gain horn; then second, to match that received by the large antenna. The resulting difference in precision attenuator settings gave the uncorrected gain difference between the two antennas.

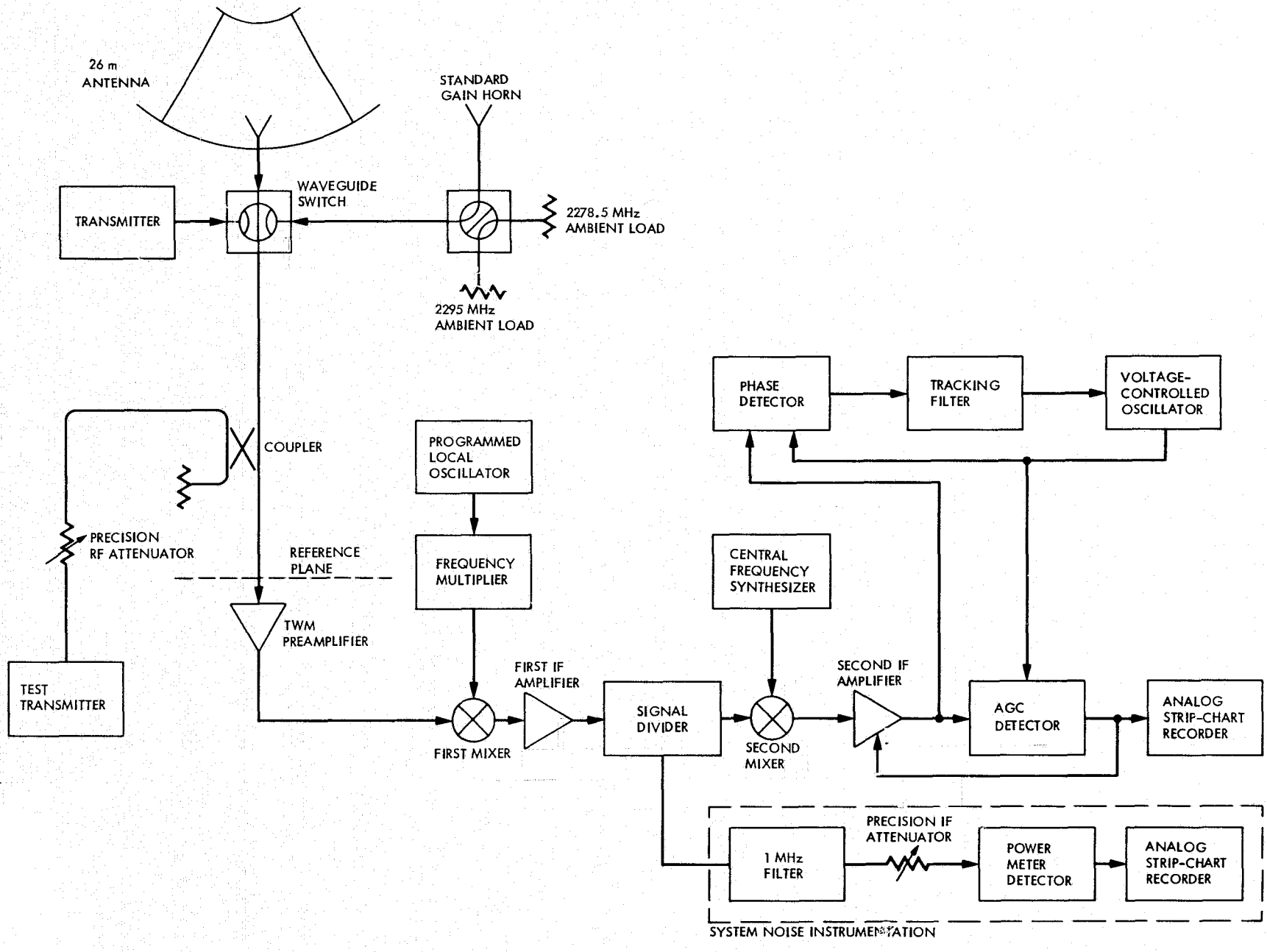

Fig. 3-1. Master Station Block Diagram Gain Transfer Calibration System

The actual sequence was as follows (Figs. 3-2 and 3-3):

(1) Using the large antenna, the receiver was phase-locked to the far field beacon, the antenna boresighted, and the AGC voltage was recorded.

(2) The receiver was retuned to the injected test signal (both the test signal and the far field beacon were left on at all times, enhancing stability) and this signal was adjusted to slightly above and slightly below the same level as previously recorded. These levels were recorded. (The reason for adjusting slightly above and below was that the attenuator used was a digital type and could not, in general, be adjusted to exactly coincide with the beacon signal. By deliberately adjusting above and below, a simple post-interpolation to the exact value was possible.)

(3) Using the gain standard horn, the receiver was phase-locked to the far field beacon and the AGC voltage was recorded.

(4) The receiver was then returned to the test signal, and this signal was again adjusted slightly above and below the level recorded in step 3 and each level was recorded.

The gain of the large antenna could then be determined (to a first order) by the algebraic sum of the gain of the gain standard horn, the test signal attenuator difference between steps 2 and 4, and the additional loss in the waveguide run connecting the gain standard horn to the preamplifier.

The reason for using the precision attenuator in a seemingly indirect way -- operating on the local test signal rather than directly manipulating the level of the far-field beacon when receiving on the large aperture -- was primarily to eliminate the potentially large error source due to receiver nonlinearity. In principle, the measurement could have been made by placing the variable attenuator in the receiving path, but this would have required that the preamplifier-receiver have well-behaved linearity. It was felt that determining the precise preamplifier-receiver response would have been more difficult than using the test signal technique selected, which placed no requirement on preamplifier-receiver linearity. The absence of a linearity requirement can be seen by noting that the entire preamplifier-receiver chain was used simply as a level comparator between steps A and B (see previously described test sequence) and subsequently between steps C and D, but not between steps A and C or B and D, which contain the large nominally 31-dB difference between the 26-m antenna and the standard horn. It was this large signal level step, which would have led to the severe linearity requirement in a more conventional test setup, that was readily handled in this case by the precision attenuator.

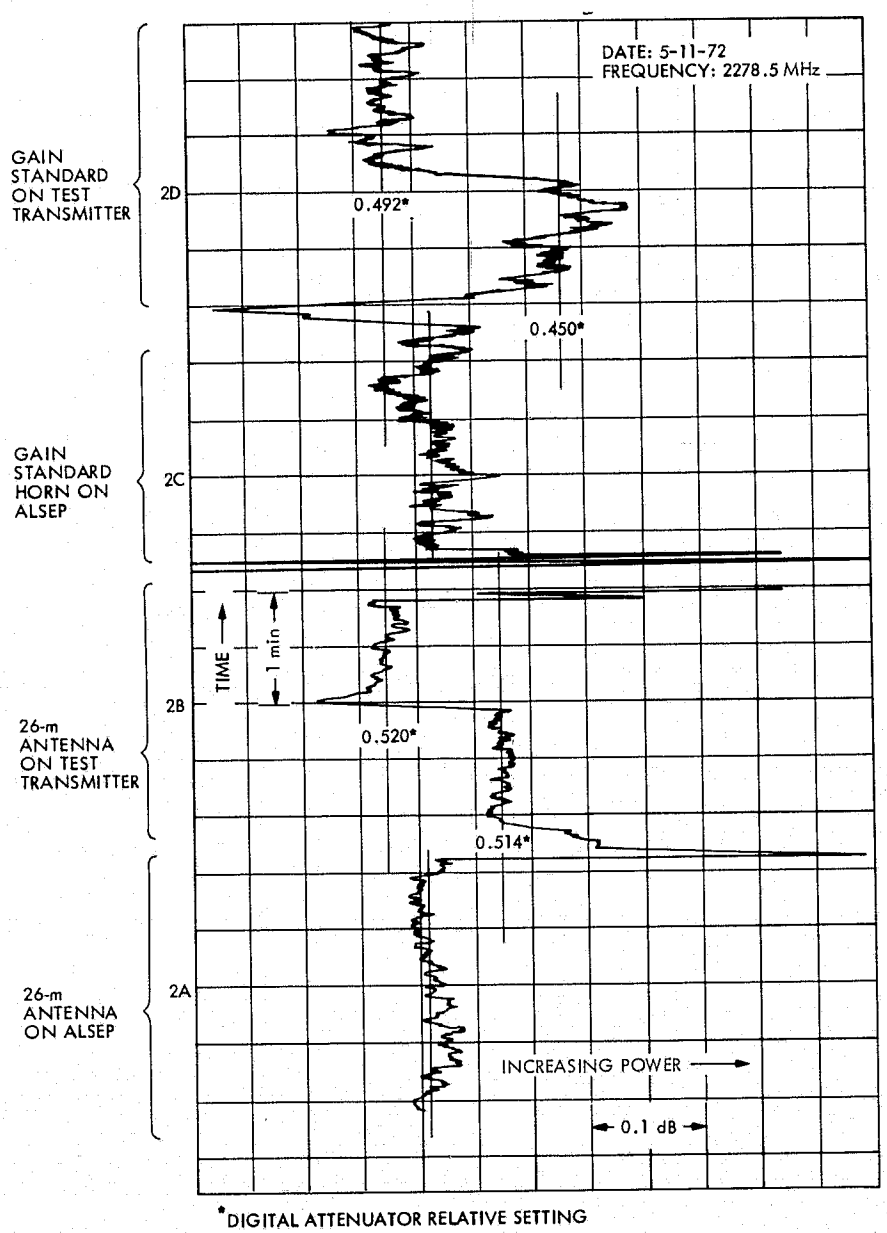

Fig. 3-2. Sample Analog Recording of ALSEP and Test Transmitter Signals

Date MAY 11, 1972 U.T

Gain Data Sheet

Operators: Rcvr MEEHAN Servo MILLER

ALSEP f_0 2,278,523,520 Hz

Strip-chart Number	Step	Ant. in use (check)	PSA Position (check)	Rcvr. Locked to (check)	Azimuth	Az. Offset	Elevation	El. Offset	Time at end of step
	A	26M. ✓	Low loss ✓	ALSEP ✓	114.6	+.059	54.3	-.032	1601
	B	26M. ✓	Low loss ✓	TEST XMTR ✓					
1	C	GSH ✓	High loss ✓	ALSEP ✓					
____	D	GSH ✓	High loss ✓	TEST XMTR ✓	116.9		55.8		1609
		Wind: direction 300 ° az, speed 5 MPH							
	A	26M. ✓	Low loss ✓	ALSEP ✓	117.6	+.053	56.3	-.032	1612
	B	26M. ✓	Low loss ✓	TEST XMTR ✓					
2	C	GSH ✓	High loss ✓	ALSEP ✓					
____	D	GSH ✓	High loss ✓	TST XMTR ✓	119.5		57.5		1620
		Wind: direction ✓ ° az, speed 0 MPH							
	A	26M. ✓	Low loss ✓	ALSEP ✓	122.9	+.053	59.5	-.032	1630
	B	26M. ✓	Low loss ✓	TEST XMTR ✓					
3	C	GSH ✓	High loss ✓	ALSEP ✓					
____	D	GSH ✓	High loss ✓	TEST XMTR ✓	125.5		60.8		1638
		Wind: direction ✓ ° az, speed 0 MPH							

COMMENTS: STEPS A+B = 0.1V
" C+D = 1V

Fig. 3-3. Sample Gain Comparison Data Sheet

C. Equipment

The large antenna that was measured was a 26-m Cassegrain-fed paraboloid at the Goldstone Deep Space Communications Complex (DSCC) in California, known as the Venus Station or Deep Space Station 13 (DSS-13). This antenna is used primarily for research, development, and special tasks and is not normally committed to longterm operational missions. The antenna had recently been fitted with a new feedcone (Ref. 3-2) and its parabolic surface reshimmed. The nominal operating system temperature (T_{OP})[8] was 16 K at zenith using a traveling wave maser (TWM) (Ref. 3-3) for the RF preamplifier. The TWM was followed by a mixer, IF amplifiers, and a phase-lock receiver designated Mod IV (Ref. 3-4) (Fig. 3-1). This was all normal station equipment.

---

[8]Appendix C, page C-8, gives the typical T_{OP} as a function of elevation angle using the 26-m antenna without a noise source in the antenna beam or a signal in the receiver passband. The zenith T_{OP} using the gain standard horn was 29 K. The noise contribution of the Moon to each system (the 26-m test antenna and the reference gain standard horn) depends on the fraction of the RF beam that is subtended by the Moon. The measurement technique previously described is independent of the differing noise levels between the test and reference antennas.

Special equipment installed for the gain transfer calibration included the gain standard horn (Fig. 3-4), the horn waveguide run (Fig. 3-5) and the test signal source and its associated special attenuators and controls. The far-field beacon used was the carrier wave of the NASA lunar-based Apollo Lunar Scientific Experiment Package (ALSEP), designated ALSEP 12.

D. Special Problems

Early in the implementation phase of this effort the question of where to locate the standard gain horn, and what effect this location would have on accuracy and operations arose. In an earlier similar calibration effort at DSS 14 (Refs. 3-5 and 3-6) a horn had been placed near the feedcone exterior, but looking about 45 deg off the large antenna axis. This proved operationally cumbersome and also raised the difficult question of possible interaction between the two antennas; therefore, that method of mounting was not used for this measurement, even though a very short waveguide connection from both the standard and large antennas to the preamplifier resulted.

The idea of placing the standard horn coincident with the large antenna axis and above the subreflector was also considered but rejected because of the necessarily long waveguide run and the possibility of quasi-focussed coupling between the antennas due to the horn backlobe-paraboloid focal point juxtaposition. It was tentatively decided to place the gain standard horn axis parallel to the large antenna axis, positioned about half-way out from the center and midway between two subreflector supporting quadripod legs (Fig. 3-6). To facilitate checking for interactions between the two antennas the standard horn was mounted on rails to allow it to move about 60 cm (24 in.) axially.

It is emphasized that in the search for multipath and its correction, the power increments measured were very small. As a consequence, no conclusion was possible using a single movement of the horn axially. Rather, in each measurement case, the search continued until a clearly defined multipath, or lack of one, was evident in the data. Individual measurements were made by storing digitized receiver AGC as a function of standard horn axial position in a computer memory. This was repeated many times and the data was computer summed. The number of individual measurements of AGC versus axial position necessary to satisfy the criteria varied from 25 to 64 two-way axial passes of the standard horn on its mounting rails.

Initial tests for multipath showed about 0.15 dB peak-to-peak interaction. Investigation to determine the sources of this interaction was fruitful. Two major sources were identified. First, not unexpectedly, some RF energy from ALSEP was reflecting off the quadripod legs into the first sidelobe of the standard horn. Second, the antenna-select waveguide switch, when positioned for gain standard horn use, simultaneously terminated the large antenna in an incidental short circuit at a transmitter-select switch farther down in the system. The energy received from ALSEP by the large antenna then would reflect off this short and reilluminate the large antenna allowing some energy to enter the gain standard horn sidelobes.

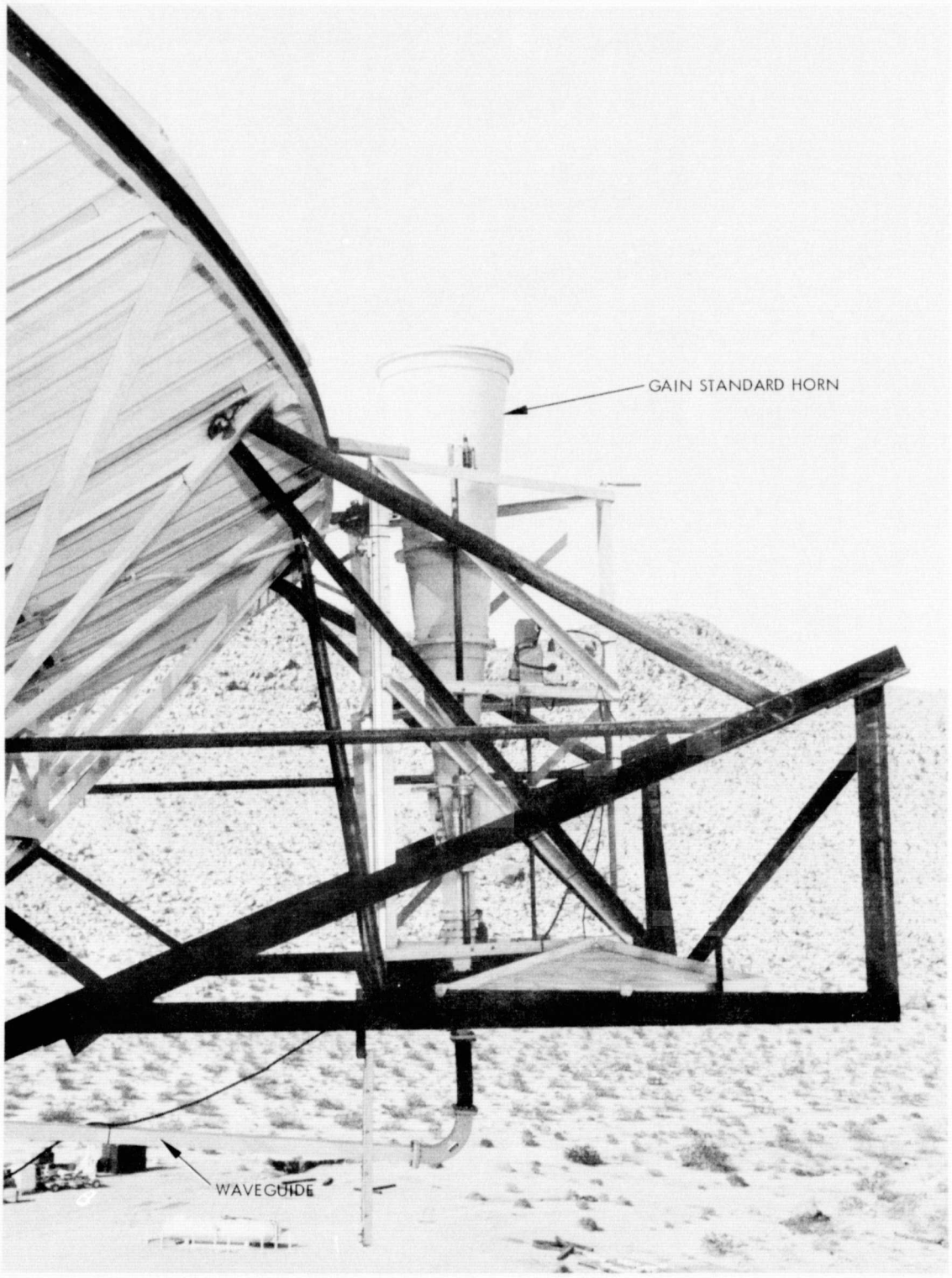

Fig. 3-4. Working Gain Standard Horn Installation on 26-m Master Station

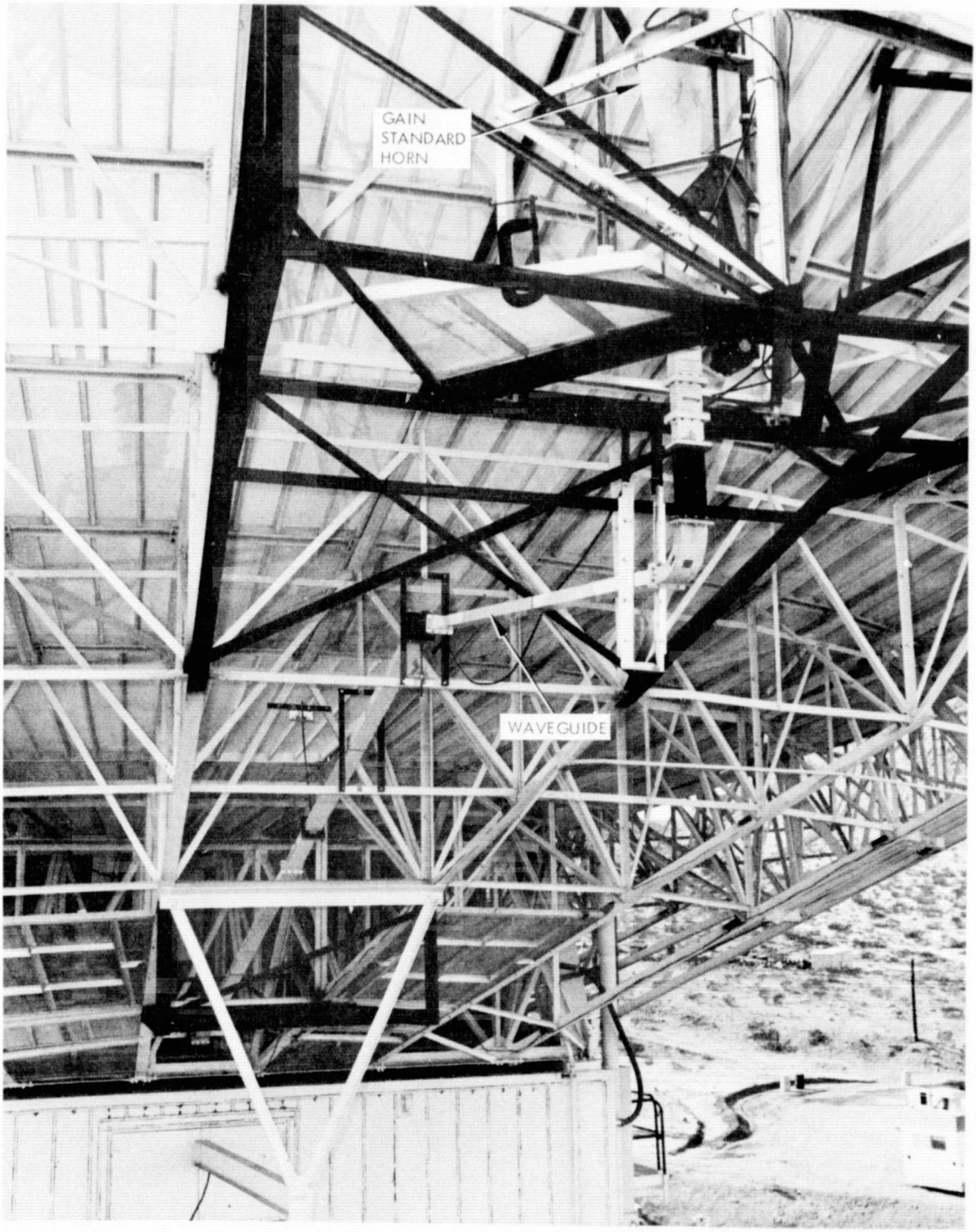

Fig. 3-5. Waveguide Run From Gain Standard Horn

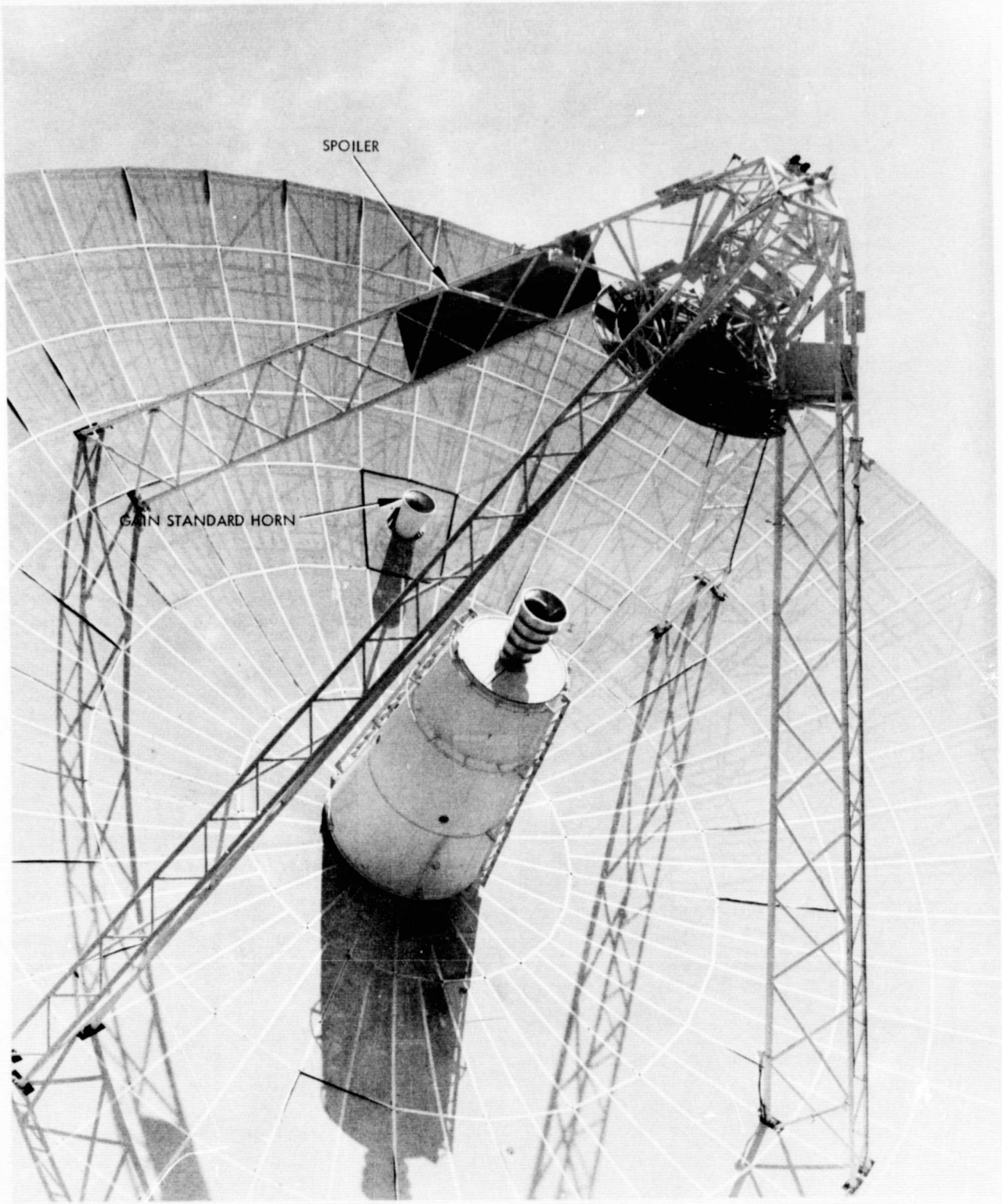

Fig. 3-6. Gain Standard Horn Mounted Within the 26-m Aperture (Oct. 1971)

By substituting a waveguide termination in place of the incidental short and placing metal reflector "spoilers" on the quadripod legs (Figs. 3-6 and 3-7) these multipath sources were reduced. Subsequent measurements showed about 0.07 dB peak-to-peak interaction.

To further reduce this multipath situation, the gain standard horn was remounted just outboard of the edge of the large antenna (Figs. 3-4 and 3-8) and the multipath tests repeated. Without either the spoilers or the waveguide termination, the multipath phenomenon was not discernible at the limits of resolution, about 0.03 dB. All gain comparison measurements were then made using this mounting location, in the mid-axial position. Because of our experience, accumulated during the above multipath tests at two antenna-mounted locations, and because of the previous conservatism especially seen in defining the gain tolerance of the working standard horn, we maintain the working standard horn gain (in situ) is identical to the value previously given, and with essentially identical tolerance, except for the multipath resolution difficulty, which is minor.

The calibration of the long waveguide run from the standard horn to the TWM preamplifier also posed a special problem. Conventional insertion loss techniques (Ref. 3-7) would have been cumbersome. A method that had been recently developed by Dr. Glenn Engen at the National Bureau of Standards (Ref. 3-8) was selected as best meeting the requirements. Before measuring the loss, the reflection coefficient of the large antenna was measured (at the TWM reference flange) and the complete gain standard horn and waveguide run system was tuned to the identical value. (The intent of this step was to reduce the comparison mismatch error to zero in the subsequent measurements.) The insertion loss value measured for the waveguide run was 0.268 ± 0.0054 dB, 3σ.

E. Precision Attenuators

The accuracy of the attenuators used to compare the power gain of the gain standard horn to the large antenna (via the locally injected test transmitter) were of prime importance. The method was to use RF attenuators, one fixed switchable step attenuator to cover the nominal difference between the two antennas and one variable attenuator to act as a high resolution vernier-type. The first was designated the precision switchable attenuator and the second the digital attenuator.

1. Precision Switchable Attenuator

The nominal gain difference between the standard gain horn and the large antenna was 31 dB. What was needed was a reliable highly repeatable, step attenuator capable of being remotely controlled. This was achieved by using a specially constructed 31-dB directional coupler and a switch, all in waveguide (Figs. 3-9 and 3-10). This unit was calibrated for differential path loss by NBS in Boulder, Colorado. The value was 31.30 dB with an uncertainty of ± 0.050 dB, 3σ.

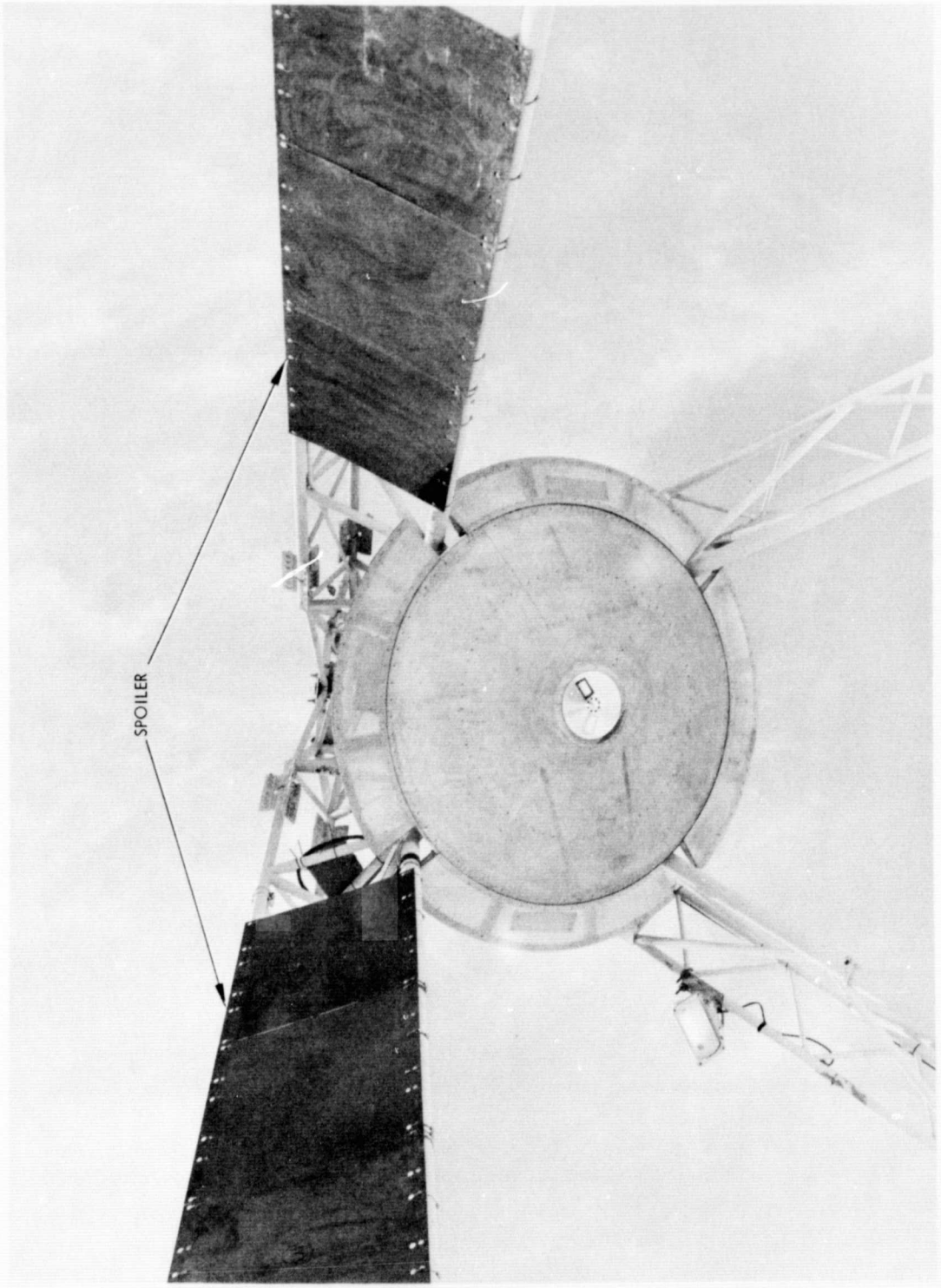

Fig. 3-7. Antenna Subreflector and Quadripod Structure With "Spoilers"

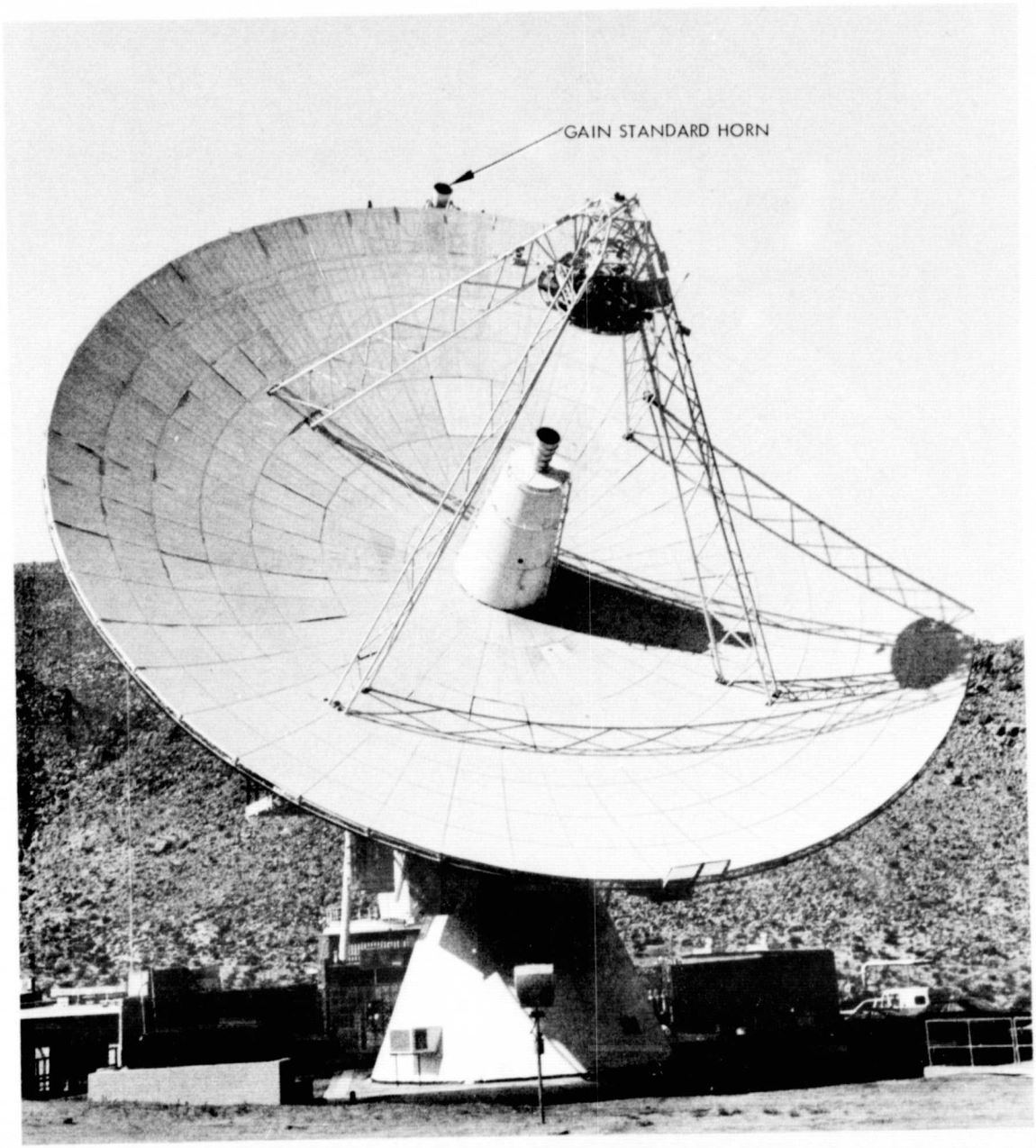

Fig. 3-8. Gain Standard Horn Mounted at Edge of 26-m Aperture (Feb. 1972)

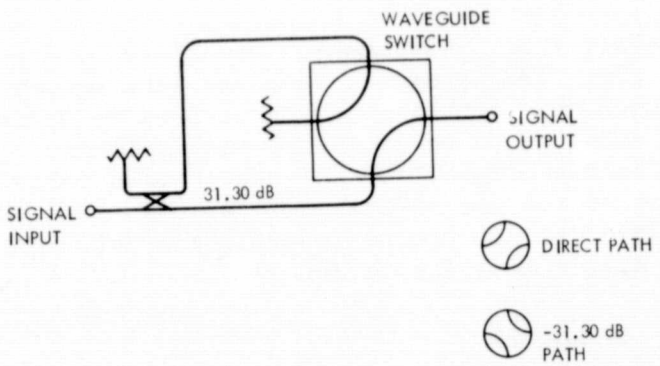

Fig. 3-9. Precision Switchable Attenuator Diagram

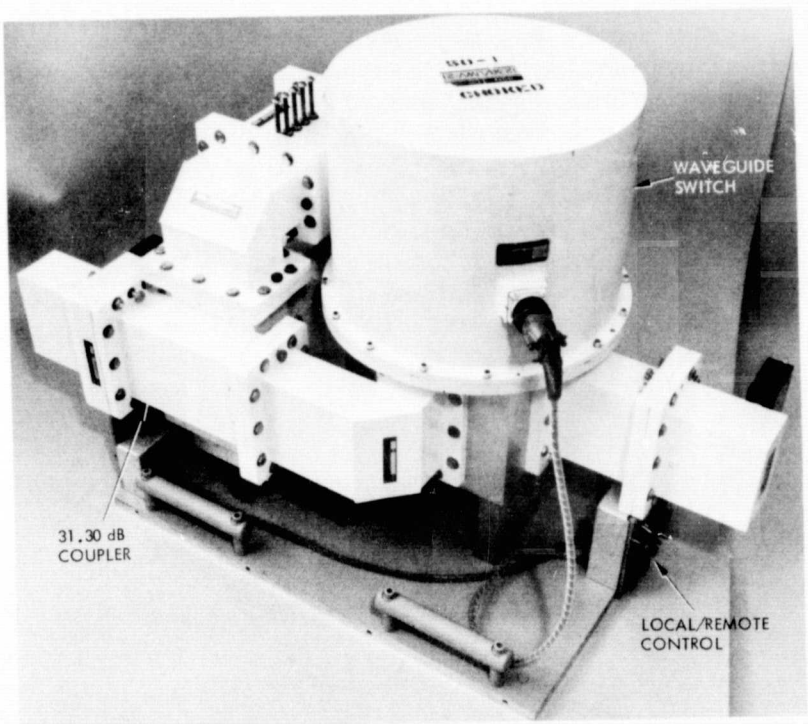

Fig. 3-10. Precision Switchable Attenuator

2. Digital Attenuator

This device (Fig. 3-11) can be described as a pulsegate carrier-level attenuator. The RF signal from the test transmitter was passed through a PIN diode modulator that was driven hard-on or hard-off by a pulse circuit. The ratio of off-time to on- plus off-time determined the average power in the received carrier signal for the narrow-band phase-locked-loop microwave receiver. The device was used as a vernier attenuator with a resolution of about 0.015 dB at its nominal operating point. A full description of a similar device is given in Ref. 3-9.

F. Tracking

Tracking a lunar-based far-field beacon with a large antenna and narrowband phase-locked receiver posed additional problems compared to the technique of tracking natural radio noise sources with a wideband radiometer, as was done in the later phase of this program. The relative motion of the Earth-Moon system is much more complex than that of the Earth-celestial sphere system. This gave rise to two difficulties: (1) a special antenna-pointing program was necessary, and (2) a doppler compensating programmed local oscillator was required. The equipment involved was the normal station furnished angle-ephemeris tape reader and processor (ATP) (Ref. 3-10) for antenna pointing and a special programmed local oscillator (Ref. 3-11). Programming data for both came from a JPL computer program designated LASER 3 (Ref. 3-12), which had been developed in support of the Apollo laser retro-reflector experiment. The successful use of this equipment for the measurement was demonstrated by the fact that over a typical eight-hour track the antenna boresight offsets showed no discernible drift, and receiver phase tuning needed attention only occasionally.

Fig. 3-11. Digital Attenuator and Controller

G. Data

After the standard gain horn location was fixed, data was taken as antenna scheduling would allow. It was soon determined that the ALSEP signal became very frequency unstable during the ALSEP lunar sunrise and sunset due to thermal transients. Since a very narrow (4 Hz) phase-locked-loop bandwidth was used to improve the signal-to-noise ratio, this phenomenon was intolerable. This necessitated not scheduling tests for a 3-4 day span around the ALSEP lunar sunrise or sunset to avoid the resulting thermal transients and the associated rapid frequency excursions.

Data was taken between March and September of 1972 on an irregular basis. Critical examination of the data both before and after reduction showed that the March through May period looked best. During this period 232 individual measurement attempts were made. Fifty-nine of the measurements were rejected for various reasons before the data was reduced; data was too unstable to allow reduction, procedural steps were omitted or incorrect, equipment failures, etc. An additional 26 measurements were rejected after data reduction because their values were unreasonable by inspection or by Chauvenet's criterion (Ref. 3-13). The remaining individual data points were examined and each was given a weighting, taking into consideration the wind speed, and the system stability, as indicated on the recording, and length of time to complete a measurement. The weighting values were 1 (poor) to 3 (good). Corrections for polarization ellipticity and antenna pointing errors were applied. A sample of the raw data recording is shown in Fig. 3-2. Figure 3-3 shows a sample operational data sheet taken simultaneously with the recorded data depicted in Fig. 3-2.

H. Results

The power gain for the 26-m (DSS 13) antenna was determined by fitting a second-order polynomial to the corrected weighted data as a function of antenna elevation angle. The resulting efficiency curve is shown in Fig. 3-12. The peak efficiency was 60.61% at 35.7-deg elevation angle.[9] Based on the exact 85-ft diameter of the "26-m antenna" this corresponds to a peak power gain of 53.653 dB at 2278.5 MHz, defined at the TWM input. The results are summarized in Table 3-1, showing the parameter breakdown used to determine this value along with each associated error limit.

---

[9]This particular 26-m reflector was shimmed to produce the best fit paraboloid at a 30-deg elevation angle, according to structural-mechanical measurements.

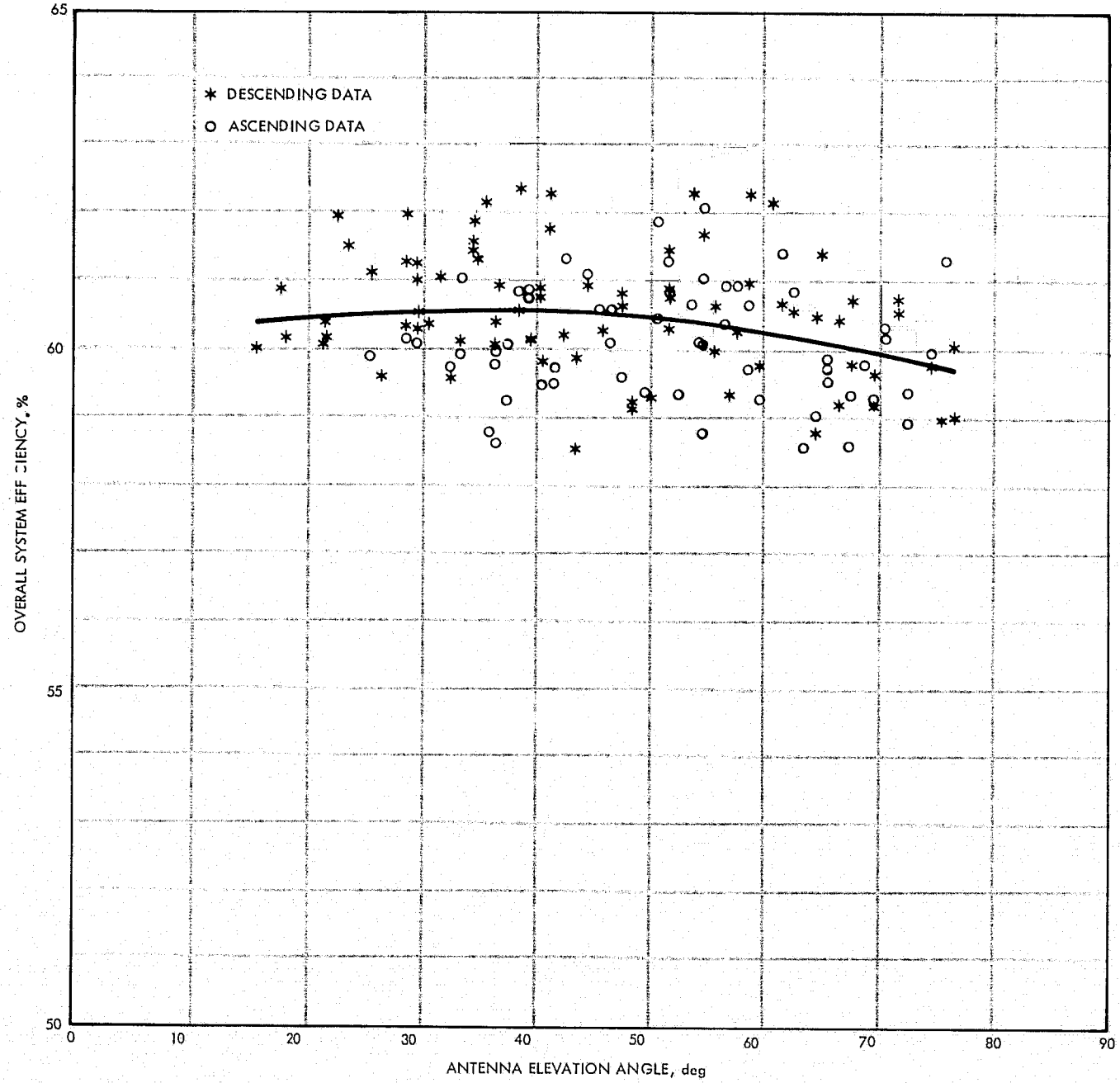

Fig. 3-12. Overall System Efficiency as a Function of Elevation Angle at 2278.5 MHz

Table 3-1. Results of DSS 13 26-m Antenna Gain Calibration, 2278.5 MHz

Parameter	Value, dB	3σ Uncertainty, dB
Measured Difference		
Precision switchable attenuator	+31.30	±0.050
Digital Attenuator		
Measurement[a]	0.650	±0.181
Calibration		±0.030
Waveguide Loss	-0.268	±0.0054
Comparison Loss (mismatch)	---	±0.005
Multipath	---	±0.015
Pointing	+0.026	±0.026
Ellipticity	+0.020	±0.045
Gain difference and accuracy	+31.728	±0.198
Gain standard horn	+21.925	±0.061
Gain of 26-m antenna[b]	+53.653	±0.207

[a]This value varies as a function of elevation angle (Fig. 3-12). The value shown is for the peak gain at 35.7-deg elevation.

[b]The gain is defined as the effective value, as measured at the TWM input flange (reference plane, Fig. 3-1).

SECTION IV

RADIO SOURCE CALIBRATION

A. INTRODUCTION

The objective of this portion of the overall program is to determine the absolute flux density of the selected natural radio noise sources within the frequency allocation (2290 to 2300 MHz) used for deep space probe communication. Once the gain of the large (master) antenna as a function of elevation is known, the absolute flux density of each of the selected radio sources may be determined from source observations. In practice the antenna gain measurements and the radio source observations were interleaved to minimize the effect of small changes (if any) in the gain of the antenna. The radio sources were selected on the basis of their qualifications as applied to the calibration of large antennas. To idealize a radio source that would be used to calibrate a large ground-based antenna, the source should have a well-known microwave spectra, a flux which is not variable with time, and the source structure should be small compared to the half power beamwidth of the observing antenna.

The radio sources selected for calibration were taken from the 3C catalog (Ref. 4-1) and the adopted source parameters are given in Table 4-1. The first four sources are intended to be used as standard calibration sources. The last source, Cassiopeia A (3C461), is not well qualified for this use but was included to relate this work to the flux density scales commonly used by the radioastronomy community.

B. OBSERVATIONS

The radio source observations used to derive the basic data were made on 66 dates from January through November 1972 with the 26-m antenna at DSS 13 which was progressively calibrated using the lunar ALSEP during the same period. The peak system efficiency at 36 deg elevation was 60.61% with a half power beamwidth of 0.33 deg or 20 arc minutes. Based on the gain measurements of the previous section, the dependence of the system efficiency with elevation angle was presented in Fig. 3-12 of the previous section. The general flatness of the gain with elevation angle indicates that the mechanical integrity of the antenna is good, which can also be seen in the axial focal length stability of the antenna.[10] The antenna receiving system with a total system operating noise temperature of 16 K consists of a right-hand circularly polarized feed with a low noise traveling wave maser. The predetection bandwidth used was 1 MHz. This predetection bandwidth with time constants on the order of 1 sec exhibited noise level jitter of 0.016 K, and the receiving system gain

---

[10] Independent tests at 3.55-cm wavelength support and extend our confidence concerning the mechanical integrity of this particular 26-m antenna.

Table 4-1. Radio Source Parameters

Source	Position (Epoch 1950)						Structure				
	Right Ascension			Declination			Type	Diameter (arc-sec)	Intensity Ratio, (%)	Spectral index N	Reference
	HR	M	S	°	'	"					
3C123	04	33	55.24	29	34	14.0	Two Points	5 5 } sep. = 23	68 32	-0.80	4-2 and 4-6
3C218 (Hydra A)	09	15	41.5	-11	53	06	Gaussian Core Halo	 45 x 15 200	 90 10	-0.92	4-3 and 4-6
3C274 (Virgo A)	12	28	18.4	12	39	43	Gaussian Core Halo	 40 x 20 400 x 460	 73 27	-0.853	4-3 and 4-7
3C405 (Cygnus A)	19	57	44.5	40	35	46	Two Points	2 2 } sep. = 120	50 50	-1.205	4-4
3C461 (Cassiopeia A)	23	21	06.8	58	32	47	Disk	276	100	-0.792	4-5 and 4-8

stability of about 0.02 dB contributes 0.080 K of noise jitter. The overall ΔT rms noise level was then 0.082 K.

Each observing session began with a check of system calibrations, including RF-IF system linearity, maser gain and effective receiver noise temperature. The system linearity was measured to a level 10 dB above the reference ambient load level. At this level the linearity was not allowed to deviate more than 0.1 dB. The procedure utilized to measure the linearity is described in Appendix B. The maser gain was peaked and measured and the effective receiver noise temperature was measured as described in the procedure of Appendix C.

The source observations consisted of two portions, the boresight determination for RF beam pointing and the measurement of the additional noise contribution of the radio source. Boresighting is the practical alignment of the peak of the antenna beam with the radio source to maximize the power transfer from source to antenna and the reliable calibration of the repeatable boresight errors. The computer program entitled CONSCAN (Ref. 4-10 and 4-11) utilized a conical scan technique that commanded the antenna pointing system and monitored the pointing errors. CONSCAN scans the RF beam of the antenna around the radio source position at a preselected radius while monitoring the total power from the receiver. Constant total power output throughout a circular scan is indicative of a zero boresight error, whereas a periodic output indication is observed when the nominal pointing coordinates are imperfect. After each scan the error was computed and the pointing commands were updated. The boresight determination described in the procedure of Appendix C outlines the manual two-axis procedure, which was discontinued as soon as CONSCAN became available. The noise contribution of the radio source was measured with the on-off technique whereby the antenna beam was stepped in position toward the source and then toward a reference position near the source. The OFF source reference positions were alternated on opposite sides of the source to account for any background sky temperature gradients around the source. The Y-factor measurements of the ON and OFF source conditions were referenced to the waveguide ambient load as described in Ref. 4-12. The step-by-step procedure recommended for these measurements, sample data sheets and sample computer processed results in the form of printed and plotted data are presented in Appendix C. The Y-factors were determined by a precision waveguide-beyond-cutoff IF attenuator and power meter detector that displays the IF power level on a stripchart recorder. The stripchart recorder was simply used as a very sensitive reference level indicator and visual integrator. The detector was operated at a constant power level for all measurements. The system noise instrumentation is included in the block diagram of Fig. 3-1.

C. CONSIDERATIONS

When making accurate absolute measurements over a large dynamic range, many potential error sources must be considered. Of two types of errors, systematic and random, the effect of systematic errors will impact the magnitude of the measurements, while the effect of random errors may be suppressed by averaging sufficient data.

1. IF Attenuator

The calibration of the precision waveguide-beyond-cutoff IF attenuator used for the Y-factor measurements was examined (Ref. 4-13). The error evaluation and operations were conducted over the attenuator range above 10 dB. The results indicated an error that had a positive linear slope of 0.002 dB per dB of range and a peak-to-peak ripple of 0.02 dB per dB. The result of a Y-factor measurement with a positive error is a noise temperature determination that is less than the true value; therefore, the correction factor to the observed noise temperatures depends on the operating range of the attenuator and is greater than unity. The precision IF attenuator correction, C_{dB}, was 0.002 dB per dB with a 1σ uncertainty of ± 0.003 dB (1σ error based on 0.02 dB P-P error). The correction coefficients with the associated uncertainties for the IF attenuator error were determined for the typical operating range of each of the sources and are given in Table 4-2 to relate the magnitudes of all the errors considered.

2. Linearity

Because of the relatively large dynamic range of system operation due to use of an ambient temperature reference noise source, the receiver linearity effects were very carefully examined. The receiver models were considered on the basis of input-output characteristics. A simple clipper model was first considered (Fig. 4-1a). The transfer characteristics give linear operation until the hard clipping limit is reached. Based on the lack of agreement with measured linearity data, the model proved to be unsuitable for this analysis. A power series cubic model was then considered (Fig. 4-1b). This model exhibits a gradual onset of saturation that is consistent with the measured data. The cubic model proved to be conservative for examining the nonlinearity in the useful range well below the 1 dB gain compression point. The mild gain compression effects in the Y-factor measurements produce optimistic results, that is, the observed source temperatures are greater than the true value; therefore the correction factor is less than unity. The uncertainty in the linearity correction based on this model is considered to be a conservative $\pm 10\%$ of the correction. The correction coefficients and the associated uncertainties are shown in Table 4-2, to show the relative magnitude of all errors considered.

3. Pointing Stability

The performance of the antenna servo system is a primary parameter to be measured and understood when observing radio sources. The pointing instabilities of the antenna system impact the radio source observation in such a way as to reduce the measured noise contribution from the source. To the extent that the pointing errors can be identified and monitored, one can adjust the measured radio source temperatures to compensate for small pointing errors.

Table 4-2. Radio Source Measurement Correction Coefficients and Associated Uncertainties

Source	IF Attenuator $C\ d_B \pm 1\sigma$	Receiver linearity[a] $C_L \pm 1\sigma$	Antenna pointing $C_p \pm 1\sigma$	Source resolution $C_R \pm 1\sigma$	Atmospheric attenuation $C_A \pm 1\sigma$ (45-deg Elevation)
3C123	1.008 ± 0.001	0.9916 ± 0.0008	1.006 ± 0.002	1.000 ± 0.000	1.016 ± 0.0022
3C218 (Hydra A)	1.009 ± 0.001	0.9916 ± 0.0008	1.006 ± 0.002	1.003 ± 0.0003	1.016 ± 0.0022
3C274 (Virgo A)	1.004 ± 0.001	0.9926 ± 0.0007	1.006 ± 0.002	1.035 ± 0.0035	1.016 ± 0.0022
3C405 (Cygnus A)	1.001 ± 0.001	0.9953 ± 0.0005	1.006 ± 0.002	1.009 ± 0.0009	1.016 ± 0.0022
3C461 (Cassiopeia A)	1.001 ± 0.001	0.9971 ± 0.0003	1.006 ± 0.002	1.023 ± 0.0023	1.016 ± 0.0022

[a] An error analysis established that correction factors for mild receiver nonlinearity are less than unity for the system and sources selected for calibration in this program. However, the reader is cautioned that, in general, the correction factor may be either greater or less than unity, depending on the relationship of the operating system noise levels (on-and-off source) and the thermal noise standard (an ambient load was used in this program).

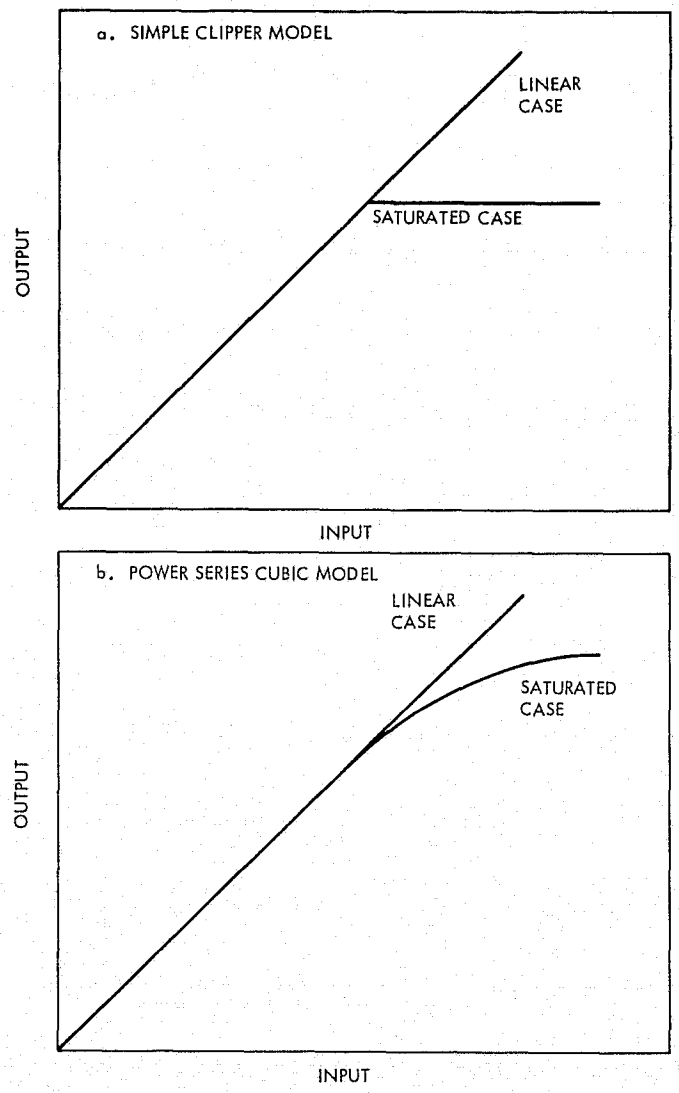

Fig. 4-1. Receiver Linearity Models

The boresight characteristics of the 26-m antenna servo system were measured for each axis over a large range of pointing angles and these characteristics were monitored for a 2 1/2 year period as a part of a separate measurement program (Klein & Stelzried Ref. 1-1). The mean azimuth offset was +0.122 deg and the mean elevation offset was +0.014 degrees. Superimposed on these mean offsets were repeatable quasisystematic offsets, which slowly changed with azimuth and elevation, as well as a component of random tracking jitter. Typical values of these two components of the boresight error were, respectively, ~0.030 and ~0.015 deg. If radio sources are observed with the mean offset corrections without any additional boresight updating with time, the measurements of source temperatures would be systematically low by ~2 or 3% (about 0.1 dB). However, if frequent boresight checks and updates are made, the error due to boresight changes can be significantly reduced. Based on operational experience with frequent updating, the pointing accuracy of the RF beam was maintained to within $\pm$0.010 deg (1σ) of the correct boresight in each axis. For typical tracking conditions away from the local zenith, the average residual boresight uncertainty is ~0.014 deg, which is the orthogonal sum of the uncertainties for the two independent axes. This uncertainty represents the typical radius of the tracking error circle of the center of the RF beam as measured from the radio source position. For a gaussian beam with a half power beamwidth of 0.33 deg, the decrease in performance for this 0.014 degree offset from the peak of the RF beam is 0.6% (0.026 dB).

The magnitude of the typical residual boresight error with frequent offset updating was confirmed (Ref. 4-14) by a direct comparison of the results of drift curve measurements and ON-OFF measurements of several radio sources for large ranges of azimuth and elevation angles. The drift curve technique, which utilizes the Earth's rotation to scan the antenna beam across the source, is affected differently by boresight errors than is the ON-OFF technique. An error in the local hour angle axis appears as a shift in time of the peak of the scan; the source appears a little early or a little late in the scan. Because this time offset can be reliably measured, the hour-angle component of the boresight error can be eliminated so that the measurement is only affected by the declination component of the boresight error. If drift curves are repeated for several increments of declination, a gaussian curve can be fitted to the peaks of these response curves and the fit determines both the peak source temperature and the average boresight error along the declination coordinate. Because ON-OFF measurements are subject to tracking errors in <u>both</u> orthogonal coordinates, the typical error is expected to be $\sqrt{2}$ larger than that for drift curve measurements. The observed source temperature with the ON-OFF method are expected to be approximately 0.5% (0.022 dB) lower than the drift curve measurements. Comparative measurements between the two methods were made and it was determined that the ON-OFF results were 0.8 $\pm$0.3% (1σ) smaller than the drift curve results. This is considered excellent agreement given the uncertainties of the measurements and the confidence level in the applied correction is felt to be a conservative $\pm$30% of the correction. Therefore, the pointing correction coefficient, C_p, of 1.006 (0.026 dB) was applied to the observed source temperature with a 1σ uncertainty of $\pm$0.002. This factor has been entered into Table 4-2 for the purpose of comparison with the other errors of the measurement.

4. Source Resolution Correction

An ideal radio source to be used to calibrate large antennas should have a size and structure which approximates a point source, where a point source is defined as a source whose angular extent is much much smaller than the antenna halfpower beamwidth. Many strong radio sources have components that span several minutes of arc, a size that is not negligible compared to the narrow beamwidth of antennas of moderate size. The systematic error introduced by the partial resolution of the source could become a significant error in this program. To improve the accuracy of source observations, a model for each source was adopted and was combined with a model of the antenna beam shape to predict the systematic error due to the partial resolution of the source. The nature of the error due to the resolution of a source would cause the observed source temperature to be less than the true value therefore the correction is greater than unity. The resolution correction of each source will depend on the size and structure of the source as well as the shape of the antenna beam.

If the structure of a radio source is assumed to have a disk-shaped distribution of radius r, and the antenna beam shape is gaussian with a half-power beamwidth of R, the resolution correction factor, C_R, is given by

$$C_R = \frac{1}{2} \frac{\left(\frac{r}{\sigma\beta}\right)^2}{1 - \exp\left[\frac{1}{2}\left(\frac{r}{\sigma\beta}\right)^2\right]}$$

where $\sigma\beta = R/2.355$ with r and R expressed in the same units. If the source structure is considered to be two point sources of equal strength with a fixed separation, d, the resolution correction, C_R, is given by

$$C_R = \exp\left[\frac{1}{2}\left(\frac{d/2}{\sigma\beta}\right)^2\right]$$

If the source structure is approximated by a gaussian distribution, the resolution correction factor, C_R, is given by

$$C_R = 1 + \left(\frac{\sigma s}{\sigma\beta}\right)^2$$

where σ_s is the angular diameter of the source and $\sigma\beta$ has been defined above. Based on the adopted structure for each source and the corresponding dimensions presented in Table 4-1, the source resolution correction coefficients were determined and are given in Table 4-2. The confidence, based on the models adopted, is about $\pm 10\%$ of the correction (which contributes a small error to the total measurements at hand).

5. Atmosphere

The influence of the Earth's atmosphere on accurate flux density measurement may introduce a significant error into absolute flux density measurements. The attenuation, which is caused by the oxygen and water content of the atmosphere, varies with frequency, temperature, and pressure as well as the composition of the atmosphere. At higher frequencies the oxygen and water content of the atmosphere are the principal components causing atmospheric attenuation. The variability of the water content of the atmosphere with time and pointing angles makes the atmospheric loss determination most difficult to the point of impairing the accuracy of the measurements. At S-band frequencies, the oxygen content of the atmosphere is the dominant component causing the atmospheric attenuation. For elevation angles above 15 deg, the loss through the atmosphere can be adequately modeled as proportional to a cosecant function of the elevation angle. The zenith atmospheric attenuation for various atmospheric conditions typical of the Goldstone DSCC area were adopted from Ref. 4-15. The normally clear atmosphere at S-band accounts for 0.04 dB of attenuation with an additional 0.02 dB contributed by a condition described as lightly cloudy. The radio source observations were conducted over a period of many months during various atmospheric conditions, but any observations taken during periods of heavy clouds were not considered for this program. The nominal atmospheric attenuation, L_o, was assumed to be 0.05 dB with a tolerance of ± 0.02 dB to cover the range of atmospheric conditions. The atmospheric loss in dB at any given elevation, $L(\psi)$, was determined from the product of the zenith attenuation, L_o, dB and the cosecant of the elevation, ψ, by the expression

$$L(\psi) = L_o \operatorname{cosec}(\psi).$$

The atmospheric correction coefficient as a function of elevation angle is given in Fig. 4-2. To emphasize the magnitude of the correction and the associated uncertainty, the correction coefficient at 45 deg is given in Table 4-2 for comparison with the other corrections and uncertainties determined for the measurements. The actual corrections for the atmospheric attenuation were, of course, applied to the source measurements based on the elevation angle of the particular observation.

6. Diurnal and Seasonal Effects

The source measurements were made during both daytime and nighttime hours throughout the 11-month duration of the observing program. Examination of the data showed no evidence of a diurnal or seasonal variation of the measured source temperatures. Therefore, the combined effect of diurnal and seasonal variations (if any) are assumed to be included in the scatter of the observed source temperatures.

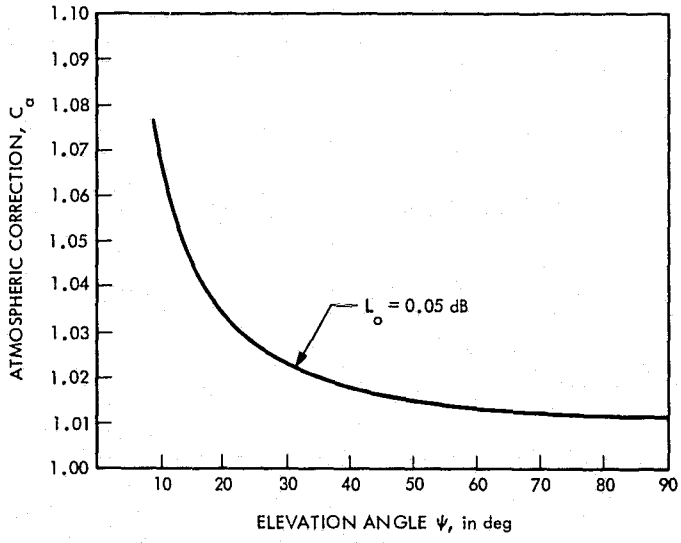

Fig. 4-2. Atmospheric Corrections as a Function of Elevation Angle

D. Results

The observed antenna temperatures were determined from independent observations of the sources and were corrected for the systematic (station-related) errors by the expression

$$\Delta T_A^* = \Delta T_A \, C_P \, C_{dB} \, C_L \, C_R$$

where ΔT_A^* is the corrected antenna temperature, ΔT_A is the measured antenna temperature, and the coefficient subscripts P, dB, L, and R identify the pointing, attenuator, receiver linearity and source resolution corrections, respectively. The typical corrected antenna temperature given in Table 4-3 is the expected increase in the operating system temperature of the 26-m antenna, due to the radio source, for an antenna-receiver system located at the Earth surface with overall 60.61% efficiency, including the normal small losses to the preamplifier input. The uncertainty of the observed antenna temperature is the measurement scatter and the observational errors associated with pointing, attenuator, receiver linearity, atmosphere, and source resolution. In Table 4-3 the source temperature, T_S, is the noise power available outside the earth atmosphere which an ideal 100% efficient 26-m antenna would observe. The source temperature for each source has been corrected for the changes in the antenna efficiency and atmospheric attenuation with elevation angle by the expression:

$$T_S = \frac{\Delta T_A^*(\psi)}{\eta(\psi)} C_A(\psi)$$

where $\eta(\psi)$ is the overall antenna efficiency, and $C_A(\psi)$ is the atmospheric correction coefficient. The uncertainty associated with the source temperature includes the uncertainties of the corrected antenna temperature, master antenna gain, and the atmospheric correction. The absolute source flux density, S, was finally determined from the source temperature as

$$S = \frac{2k\ T_S}{A_p}$$

where S is the flux density in $W^1m^{-2}\ Hz^{-1}$, A_p is the cross sectional area of the antenna in square meters and k is Boltzmann's constant ($1.380622 \times 10^{-23}\ W^1\ H_Z^{-1}K^{-1}$). The "26-m antenna" diameter is physically 85 ft exactly.

The 3σ source temperature measurement precisions and accuracies are presented in Table 4-4. The largest uncertainty of the source observations was the measurement scatter ranging from ± 1 to 3% (3σ) including the uncertainty of the ambient load as referenced to the input of the maser amplifier. The range was a function of the strength of the source and the quantity and quality of the measurements. The uncertainty of the corrections applied to the measurements ranged from ± 0.7 to 1% 3σ, and indicated a high confidence level in those corrections as they relate to the master station observations. The uncertainty of the atmospheric correction at zenith was less than 0.5%. The accuracy of the atmospheric correction was a large contributor of the total uncertainty of the total applied correction. The total uncertainty of the source observations ranged from less than 1.5% to slightly more than 3% (3σ). This range resulted from the actual root sum square of measurement scatter and correction uncertainties applied on a source by source basis (i.e., the source measurement with the lowest antenna temperature measurement scatter may not have had the lowest correction factor uncertainty.)

The absolute flux density of five radio sources and the 1σ uncertainty are presented in Table 4-3. The uncertainty in the absolute flux density is less than 2% (1σ) for all of the sources observed where the master antenna absolute gain determination and the source temperature measurements contributed approximately 1.5 and 1.0%, respectively. A program result of ± 0.22 dB (± 5 %), 3σ uncertainty in calibrated flux density has been achieved, with the unique direct use of a calibrated large aperture as a key program feature. The total correction factors applied to the source observations were less than 5% with the associated uncertainty contribution being a small portion of the overall uncertainty of the measurements. The flux density of Cassiopeia A determined by these measurements agrees to within about 1% of the translated flux density reported by Dent, Aller, and Olsen in Ref. 4-17. The ratios of 3C123 and Hydra A (3C218) to Virgo A (3C274) are in excellent agreement with the measurements reported by Klein and Stelzried in Ref. 1-1; however, the assumed value for Virgo A

Table 4-3. Antenna Temperatures and Absolute Flux Density at 2278.5 MHz

Source	Typical corrected 26-m antenna temperature[a] $\Delta T_A^* \pm 1\sigma$, K	100% Efficient 26-m antenna source temperature[b] $T_S \pm 1\sigma$, K	Flux density[c] $S \pm 1\sigma$ (JY)[d]
3C123	3.56 ± 0.038	5.96 ± 0.117	31.2 ± 0.61
3C218 (Hydra A)	3.06 ± 0.030	5.14 ± 0.097	26.9 ± 0.51
3C274 (Virgo A)	15.6 ± 0.16	26.1 ± 0.50	136.5 ± 2.6
3C405 (Cygnus A)	102 ± 0.44	171 ± 2.9	895 ± 15
3C461 (Cassiopeia A)[e]	175 ± 1.0	293 ± 5.0	1534 ± 27

[a]At the earth's surface; typically 45-deg elevation; rounded values

[b]Above the Earth's atmosphere; rounded values.

[c]Flux density based on exact value, then rounded.

[d]JY ≡ JANSKY = 10^{-26} $W\,m^{-2}\,Hz^{-1}$

[e]Flux density known to decrease approximately 1% per year (observation epoch 1972.6)

as reported by Baars and Hartsuijker in Ref. 4-7 and adopted by Klein and Stelzried is about 3% higher than the flux determined by these measurements.

The sources, 3C123, Hydra A, Virgo A and Cygnus A are all recommended as good gain standard sources for work with uncalibrated 26- and 34-m antennas at S-band. With careful attention to the measurement details, the 26 m DSN antennas can achieve an overall gain calibration accuracy of ±0.23 dB compared with the program goal of ±0.30 to 0.40 dB. The sources, 3C123, Hydra A (3C218) and Virgo A (3C274) are recommended as good sources for determining the gain of the DSN 64-m antennas at S-band. Due to the source size and structure, the resolution corrections and associated uncertainties of the other sources are considered large and would impact the accuracy of the measurements; therefore, those sources are not recommended for the larger antennas.

Table 4-4. Source Temperature Measurement Precision and Accuracies

Source of uncertainty	Uncertainty[1], 3σ	
	dB	Percent
Measured antenna temperature	$\pm$0.046 to $\pm$0.136	$\pm$1.07 to $\pm$3.18
Antenna temperature correction	$\pm$0.031 to $\pm$0.042	$\pm$0.72 to $\pm$0.97
Atmospheric correction (zenith)	$\pm$0.020	$\pm$0.47
Total[2]	$\pm$0.064 to $\pm$0.142	$\pm$1.48 to $\pm$3.30

[1] Range of values due to source magnitude and/or data quality.

[2] Total with respect to individual sources.

E. Application to Operational DSN

With the development of a detailed DSN procedure describing the steps necessary to insure successful user station observations of a radio source, the absolute antenna gain may be determined. This procedure, presented in Ref. 4-17, uses the simple half-power-point boresight technique to assure proper RF beam pointing and the ON-OFF source observation technique utilizing Y-factor measurements to determine the observed antenna temperature increase due to the source in the antenna beam. Using the equations given in Section D, the corrected antenna temperature and thence either η or η/Ca may be formed. For DSN use, the effective efficiency is, in fact η/Ca; that is, including the degradation of the normal atmosphere. The absolute flux density of the calibrated radio sources is the basic standard for this determination of antenna gain. Secondary standards are the user station noise temperature reference (waveguide ambient load) and the variable IF attenuator.

For DSN use, the S-band gain specification is required to be within the operating bandwidth of the normal station tracking receivers (2290 to 2300 MHz); therefore, the source flux density calibrations of the previous section must be translated in frequency. The microwave spectrum of the radio sources can be approximated by a power law where the flux density S, is related to frequency f, by the expression $S \propto f^N$, where N is the spectral index of the source. Due to spectrum curvature of the flux density of some radio sources, the flux density translation with frequency over a wide range becomes inaccurate. However, the translation from 2278.5 to 2295 MHz is so small that the error introduced is negligible compared to other errors in the measurement. The translated flux densities

at 2295 MHz are presented in Table 4-5 with the 100% source temperatures to be used to determine the efficiency of DSN 26-, 34- and 64-m antennas. The source resolution correction factors for the five calibrated sources are given in Table 4-6 to aid in selecting a source.

1. Achievable Accuracy

The achievable accuracy of DSN operational radio source observations is directly related to the precision (data scatter) obtainable from use of the presently available DSN non-gain stabilized radiometers, to operating techniques, and to a lesser extent, to the accuracy of a few key operating system components. Consider for the moment, two modes of operation. The first is a single observation of a radio source with a minimum level of evaluation of the user system uncertainties. With typical scatter and infrequent calibrations of the system components such as receiver linearity, pointing performance, IF attenuator calibration and partial resolution of the radio source, the overall accuracy of the observational step (taken alone) is estimated to be about ± 0.30 dB (3σ). The second mode of operation would entail several observations of a radio source with a systematic error evaluation comparable to the quality achieved at the master station. The achievable accuracy of such observations, taken alone, would be comparable to the ± 0.07 dB (3σ) obtained during the calibration observations of the sources at the master station, as reported in the previous section.

2. Results

The estimated accuracy of the user station radio source observational step ranges from 0.30 to 0.07 dB (3σ). The preferred method is the full systematic error evaluation with the determination of corrections as well as associated uncertainties. The cost of more precise measurements is naturally a greater expenditure of user station time. The overall absolute antenna gain uncertainty of the user station will then be the incoherent sum of the accuracy of user station observations, ± 0.30 to 0.07 dB, and the absolute flux density uncertainty of the radio source observed, ± 0.22 dB, resulting in a range from ± 0.37 dB to ± 0.23 dB (3σ).

Table 4-5. Absolute Flux Density and Antenna Temperatures at 2295 MHz

Source	Flux density $S \pm 1\sigma$, JY	100% Efficient antenna T_S, K		
		26-m	34-m	64-m
3C123	31.0 ± 0.61	5.92	10.2	36.2
3C218 (Hydra A)	26.7 ± 0.51	5.10	8.78	31.2
3C274 (Virgo A)	136 ± 2.6	25.9	44.6	158
3C405 (Cygnus A)	887 ± 15	169	292	1034
3C461 (Cassiopeia A)[1]	1525 ± 27	291	502	1777

[1]Flux density known to decrease approximately 1% per year (observation epoch 1972.6)

Table 4-6. Source Resolution Corrections

Source	Source resolution corrections $C_R \pm 1\sigma$		
	26 m	34 m	64 m
3C123	1.000	1.001 ± 0.0001	1.003 ± 0.0003
3C218 (Hydra A)	1.003 ± 0.0003	1.007 ± 0.0007	1.017 ± 0.0017
3C274 (Virgo A)	1.035 ± 0.0035	1.076 ± 0.0076	1.173 ± 0.017
3C405 (Cygnus A)	1.009 ± 0.0009	1.015 ± 0.0015	1.035 ± 0.0035
3C461 (Cassiopeia A)	1.023 ± 0.0023	1.040 ± 0.0040	1.093 ± 0.0093

SECTION V

CONCLUSIONS AND RECOMMENDATIONS

The JPL S-band Antenna Gain Calibration Program has stairstepped from a very high accuracy gain standard horn calibration, through a large aperture master station transfer calibration using the CW signal from the ALSEP located on the Earth's moon, to absolute flux density calibrations of five selected galactic and extragalactic natural radio sources. Included in the program was a study and estimate of the achievable absolute gain accuracy applying the calibrated sources to a worldwide network of large ground antennas. The results show high confidence accuracies of ± 0.23 to ± 0.37 dB are possible, depending primarily on measurement scatter of the returned field data, and to a lesser extent on evaluation of a few key parameters at each user station.

Considerable attention to detail was exercised throughout the various steps of the program, and most conservative error estimates have been made. Refinement (in the sense of better accuracy) is possible with further work, for some portions of the program, especially the gain standard horn calibrations that were actually done in three different and independent ways. Advantage has not been taken of the independent methods used when quoting a final horn gain accuracy. In the same manner, an exhaustive post calibration of the working unit (field-installed) standard horn used was conducted, with several "loop-closing" internal consistency checks. Nonetheless simple-sum uncertainty totals for the accuracies achieved in the horn calibration phase of the work are quoted. Suppressed-sidelobe standard gain horns are certainly recommended for future work of a similar nature.

In that phase of the program that obtained the calibration of the master station, we again proceeded with a great deal of attention to detail. For example, small multipath interactions between the standard and test antenna were extensively examined and ultimately eliminated. Finally, great care was taken to understand the impact of the receiver linearity on overall accuracy in the program phase that determined absolute source flux density of the natural sources; receiver linearity again becomes important in the user-station final phase.

The reader will notice that measurement scatter (data <u>precision</u>) as contrasted with systematic <u>accuracy</u> sources of error weigh in as large contributors to the final results in this program. For that reason, possible future efforts of a similar nature could benefit by the experience we gained herein, and planning for a possible improvement in the balance among error sources might be a worthwhile first consideration.

Given additional time, improvements in three major areas of the program could be accomplished. In the area of gain standard horns, advantages of the three independent calibration methods could significantly reduce the horn gain uncertainty. In the area of the master station calibrations, automation of the gain measurement would improve the measurement scatter as well as ease the repetition of the measurement. A more careful examination of the ellipticity problem among the ALSEP

antenna, gain standard horn, and 26-m antenna would reduce the needed correction and associated uncertainty as well as reducing the scatter of the gain measurement. Improvement in the radio source observation measurements would result from automation of the radio source observations. Improved weather monitoring during the measurements would reduce the uncertainty of the atmospheric corrections. The use of a gain stabilized radiometer, such as a noise adding radiometer (NAR), would reduce the measurement scatter and would lend itself well to automation as well as further easing the repetitive nature of the radio source observations. The list of radio sources should be expanded to increase the availability of the calibrated sources to the user stations.

As the utilization of large aperture antennas moves toward higher frequencies (e.g., X-band and beyond), accurately calibrated radio sources will obviously be necessary. If similar S-band techniques are used at X-band, antenna pointing and far-field CW signal source selection need special attention. An X-band program should be initiated to further develop gain standards (and thereby calibrated galactic and extragalactic natural radio sources) as well as to improve measurement equipment and procedures to ensure comparable accuracies at the higher frequencies to support requirements of future missions.

REFERENCES

1-1. Klein, M. J., Stelzried, C. T., "Calibration Radio Sources for Radioastronomy: Precision Flux Density Measurements at 2295 MHz," Astronom. J., Vol. 81, No. 12, pp. 1078-1083, 1976.

2-1. Potter, P. D., "A New Horn Antenna With Suppressed Sidelobes and Equal Beamwidth," Microwave J., pp. 71-78, June 1963.

2-2. Ludwig, A. C., "Antenna for Space Communication," Space Programs Summary 37-36 Vol. IV, pp. 249-255, Jet Propulsion Laboratory, Pasadena, Calif., Dec. 31, 1965.

2-3. Ludwig, A., Hardy, J., Norman, R., Gain Calibration of a Horn Antenna Using Pattern Integration, Technical Report 32-1572, Jet Propulsion Laboratory, Pasadena, Calif., Oct. 1, 1972.

2-4. Ludwig, A. C., and Norman, R. A., "Correction Factor for Near-Field Horn Antenna Gain Measurements," Space Programs Summary 37-57, Vol. II, pp. 104-108, Jet Propulsion Laboratory, Pasadena, Calif., May 31, 1969.

2-5. Norman, R. A., "Correction Factors for Near-Field Horn Antenna Gain Measurements," Space Programs Summary 37-63, Vol. II, pp 34-35, Jet Propulsion Laboratory, Pasadena, Calif., May 31, 1970.

2-6. "S-band Antenna Gain and Pattern Calibration," Space Programs Summary No. 37-22, Vol. III, pp 11-16, Jet Propulsion Laboratory, July 31, 1963.

2-7. Ludwig, A. C., "Gain Computations From Pattern Integration," IEEE Trans. AP-15, No. 2, pp 309-311, March 1967.

2-8 Ludwig, A. C., "Computer Programs for Antenna Feed System Design and Analysis," Technical Report 32-979, Vol. II, Jet Propulsion Laboratory, Pasadena, Calif., April 15, 1967.

2-9. Bathker, D. A., "Efficient Antenna System: Evaluation of 4.671 λ Aperture dual Mode Horn," Space Programs Summary 37-47, Vol. II, pp. 73-85, Jet Propulsion Laboratory, Pasadena, Calif., Sept. 30, 1967.

2-10. Stelzried, C. T., and Otoshi, T. Y., "Radiometric Evaluation of Antenna Feed Component Losses," IEEE Trans. Instrumen. Meas., Vol. IM-18, No. 3, p. 172, September 1969.

2-11. Levy, G. S., Bathker, D. A., Higa, W. H., and Stelzried, C. T., "The Ultra Cone: An Ultra-Low-Noise Space Communication Ground Radio-Frequency System," IEEE Trans. Micro. Theor. Tech., Vol. MTT-16, No. 9, p. 596, September 1968.

2-12. Levy, G. S., Bathker, D. A., and Ludwig, A. C., "Efficient Antenna Systems: Gain Measurements of The Advanced Antenna System Using Surveyor I Signals," The Deep Space Network, Space Programs Summary 37-44, Vol. III, pp. 100-105, Jet Propulsion Laboratory, Pasadena, Calif., March 31, 1967.

2-13. Yaghtian, A. D., "Upper-Bound Errors in Far-Field Antenna Parameters Determined From Planar Near-Field Measurements," NBS Technical Note 667, October 1975.

2-14. Newell, A. C., Baird, R. C., Wacker, P. E., "Accurate Measurement of Antenna Gain and Polarization at Reduced Distances by an Extrapolation Technique," IEEE Trans. Ant. and Prop., Vol. AP-21, pp. 418-431.

2-15. Otoshi, T. Y., and Stelzried, C. J., "Improved RF Calibration Technique: WR 430 Waveguide Precision Rotary-Vane Attenuator Calibration," Space Programs Summary 37-46, Vol. III, pp. 73-82, Jet Propulsion Laboratory, Pasadena, Calif., July 31, 1967.

3-1. Wait, D. F., Daywitt, W. C., Kanda, M., and Miller, C. K. S., A Study of the Measurement of G/T Using Cassiopeia A, Technical Report No. ACC-ACO-2-74, National Bureau of Standards, Boulder, Colo., June 1974.

3-2. Jackson, E. B., Gosline, R. M., and Kolby, R. B., "DSS-13 Operations: System Improvements (Antenna Systems)," in Space Programs Summary 37-59, Vol. II, pp. 93-95, Jet Propulsion Laboratory, Pasadena, Calif., Sept. 30, 1969.

3-3. Reid, M. S., "Improved RF Calibration Techniques: System Operating Noise Temperature Calibrations," The Deep Space Network Progress Report 32-1526, pp. 123-128, Jet Propulsion Laboratory, Pasadena, Calif., Aug. 15, 1972.

3-4. "Mod IV Planetary Radar Receiver," Space Programs Summary 37-21, Vol. III, pp. 49-61, Jet Propulsion Laboratory, Pasadena, Calif., May 31, 1963.

3-5. Levy, G. S., Bathker, D. A., and Ludwig, A. C., "Efficient Antenna Systems: Gain Measurements of the Advanced Antenna System Using Surveyor I Signals," Space Programs Summary 37-44, Vol. III, pp. 100-105, Jet Propulsion Laboratory, Pasadena, Calif., March 31, 1976.

3-6. Levy, G. S., Bathker, D. A., Ludwig, A. C., Neff, D. E., and Seidel, B. L., "Lunar Range Radiation Patterns of a 210-Foot Antenna at S-band," IEEE Trans. Ant. Prop., Vol. AP-15, No. 2, pp.311-313, March 1967.

3-7. Otoshi, T. Y., Stelzried, C. T., "Comparisons of Waveguide Losses Calibrated by the DC Potentiometer, AC Ratio Transformer, and Reflectometer Techniques," IEEE Trans. Micro. Theor. Tech., (Correspondence) Vol. MTT-18 N7, pp. 406-409, July, 1970.

3-8. Engen, G. F., "An Introduction to the Description and Evaluation of Microwave Systems Using Terminal Invariant Parameters," NBS Monograph 112, National Bureau of Standards, Boulder, Colo., October 1969.

3-9. Bunce, R. C., and Shallbetter, A. C., "Pulse-Gate Carrier Level Attenuation for Receiver Calibrations," Space Programs Summary 37-53, Vol. II, pp. 102-106, Jet Propulsion Laboratory, Pasadena, Calif., September 1968.

3-10. "Angle-Ephemeris Tape Reader and Processor," Space Programs Summary 37-18, Vol. III, pp. 40-42, Jet Propulsion Laboratory, Pasadena, Calif., Nov. 30, 1962.

3-11. Winkelstein, R., "Minicomputer-Controlled Programmed Local Oscillator," JPL Quarterly Technical Review, Vol. 1, No. 3, pp. 79-87, Jet Propulsion Laboratory, Pasadena, Calif., October 1971.

3-12. Mulholland, J. D., "User's Guide to Program LASER 3," Jet Propulsion Laboratory, Pasadena, Calif., March 1971 (JPL internal document).

3-13. Worthing, A. G., and Geffner, J., Treatment of Experimental Data, 9th edition, pp. 170-171, John Wiley & Sons, New York, 1960.

4-1. Kellermann, K. I., Pauliny-Toth, I. I. K., and Williams, P. J. S., (1969), "The Spectra of Radio Sources in the Revised 3C Catalogue," Astrophys. J., Vol. 157, pp. 1-34, 1969.

4-2. Fomalont, E. B., and Moffet, A. T., "Positions of 352 Small-Diameter Radio Sources," Astron. J., Vol. 76, No. 1, pp. 5-11, February 1971.

4-3. Fomalont, E. B., "Two-Dimensional Structures of 76 Extragalactic Radio Sources at 1425 MHz," Astron. J., Vol. 76, No. 6, pp. 513-524, August 1971.

4-4. Bridle, A. H., Davis, M. M., Fomalont, E. B., and Lequeux, J., "Flux Densities, Positions, and Structures for a Complete Sample of Intense Radio Sources at 1400 MHz," Astron. J., Vol. 77, No. 1401, pp. 405-443, August 1972.

4-5. Kanda, M., "An Error Analysis for Absolute Flux Density Measurements of Cassiopeia A," IEEE Trans. Instrumen. Meas., Vol. IM-25, No. 3, pp. 173-182, September 1976.

4-6. Kellermann, K. I., Pauliny-Toth, I. I. K., and Tyler, W. C., "Measurements of the Flux Density of Discrete Radio Sources at Centimeter Wavelengths. I. Observations at 2695 MHz (11.3 cm)," Astron. J., Vol. 73, No. 5, Part I, pp. 298-309, June 1968.

4-7. Baars, J. W. M., and Hartsuijker, A. P., "The Decrease of Flux Density of Cassiopeia A and Absolute Spectra of Cassiopeia A, Cygnus A, and Taurus A," Astron. Astrophys., Vol. 17, No. 2, pp. 172-181, 1972.

4-8. Dent, W. A., Aller, H. D., and Olsen, E. T., "The Evolution of the Radio Spectrum of Cassiopeia A," Astrophys. J., 188: L11-L13, Feb. 15, 1974.

4-9. Freiley, A. J., "Performance of DSS 13 26-m Antenna at X-band," The Deep Space Network Progress Report 42-30, pp. 113-118, Jet Propulsion Laboratory, Pasadena, Calif., Dec. 15, 1975.

4-10. Gosline, R. M., "Conscan Implementation at DSS 13," The Deep Space Network Progress Report, Technical Report 32-1526, Vol. XIV, pp. 87-90, Jet Propulsion Laboratory, Pasadena, Calif., March 15, 1973.

4-11. Ohlson, J. E., and Reid, M. S., "Conical Scan Tracking with the 64-m Diameter Antenna at Goldstone, Technical Report 32-1605, Jet Propulsion Laboratory, Pasadena, Calif., Oct. 1, 1976.

4-12. Stelzried, C. T., "Operating Noise-Temperature Calibration of Low-Noise Receiving Systems," Microwave J., Vol. 14, No. 6, p. 41, June 1971.

4-13. Stelzried, C. T., Seidel, B., Franco, M., and Acheson, D., "Improved RF Calibration Technique: Commercial Precision IF Attenuator Evaluations," JPL Technical Report 32-1526, Vol. XII, pp. 74-82, Jet Propulsion Laboratory, Pasadena, Calif., Dec. 15, 1975.

4-14. Klein, M. J., private communication.

4-15. Peifenstein, E. C., Gaut, N. E., Waters, J. W., Moran, J. M., Phase and Attenuation at S and X-band Under Various Atmospheric Conditions," Technical Report No. 13, Environmental Research and Technology, Inc., Waltham, Mass., April, 1972.

4-16. Dent, W. A., Aller, H. D., and Olsen, E. T., "The Evolution of Radio Spectrum of Cassiopeia A," Astrophys. J., 188: L11-13, February 15, 1974.

4-17. Caswell, R., "DSN Standard Test/Training Plan and Procedures," DSN Series 850, Vol. III, DSIF Standard Test Procedure No. 853-53, 2D-01: RF System Test, April 1, 1975 (JPL internal document).

APPENDIX A

NATIONAL BUREAU OF STANDARDS REPORT OF CALIBRATION, JPL/NBS GAIN STANDARD HORNS

U. S. DEPARTMENT OF COMMERCE
NATIONAL BUREAU OF STANDARDS
INSTITUTE FOR BASIC STANDARDS
BOULDER, COLORADO 80302

REPORT OF CALIBRATION

STANDARD GAIN HORNS

Jet Propulsion Laboratory
Serial Nos. 1, 2, 3, and 4

Submitted by:

Jet Propulsion Laboratory
Pasadena, California

The on-axis measurements reported here were performed at six frequencies for a pair of linearly-polarized S-band horns and a pair of circularly-polarized S-band horns. The horns are to be used as gain standard antennas to calibrate large antennas for radio astronomy measurements [1, 2]. Since a major uncertainty component in these measurements is the uncertainty in the gain standard considerable effort was expended to achieve extreme accuracy in determining their gains.

The antennas were aligned such that the axis of measurements were along the directions of maximum gain, and a modified extrapolation measurement technique[3] was used to evaluate and correct for near-zone and multipath effects in the measured data.

The following material consists of a description of the horns, a table of the measured gain values, and a summary of the sources of uncertainty in the measurements.

Both pairs of horns were designed and fabricated by JPL. The four horns are all dual-mode, conical horns with circular cross section. Horns of this type have desirable characteristics for use as feeds for large antennas. These same characteristics, low sidelobe levels and closely matched E and H plane beam widths, are also desirable for gain-standard antennas. Also, the horns have relatively small phase-error due to the small conical angle used in their design; and this results in relatively

small proximity effects (i.e. "near zone" effects) when they are being measured. The only undesirable characteristic of these horns is that they have only about a 9 percent bandwidth. The design frequency (i.e. the center frequency for the operating band) is 2295 MHz; and the horns were calibrated at the six frequencies shown in the table. For both pairs of horns, the two antennas were nearly identical. The linearly polarized horns are identified as horns number 1 and 2.

The pair of circularly-polarized horns are physically identical to the linearly-polarized pair except for the insertion of two additional parts (permanently joined into one unit) between the three-inch section of circular waveguide and the mode generator. For the circularly-polarized horns, the sequence from the waveguide transducer to the mode generator is then: three-inch circular waveguide section, circular polarizer, three-inch circular waveguide section. Horn number 3 is horn number 1 converted to circular polarization and horn number 4 is horn number 2 converted to circular polarization.

The table presents the gain for the four antennas at the six different frequencies with an estimate of the uncertainty limits for each measurement. The measurements were taken at a separation distance of 15.650 meters.

MEASURED GAINS FOR THE JPL S-BAND GAIN-STANDARD HORNS

Frequency	Gain (dB)		Gain (db)		Uncertainty
(MHz)	G_1	G_2	G_3	G_4	dB
2277.5	21.921	21.970	21.935	21.959	± .031
2282.5	21.956	22.005	21.963	21.986	± .036
2287.5	21.991	22.040	21.992	22.015	± .031
2292.5	22.015	22.065	22.012	22.033	± .036
2295.0	22.029	22.078	22.023	22.042	± .036
2297.5	22.042	22.092	22.035	22.053	± .031

A modified three-antenna method was used for the gain measurements. From the coupling equations between two antennas with finite separation, the product G_1G_2 of their gains can be determined from the frequency, separation distance, reflection coefficients, polarizations, a near-zone connection, and the insertion-loss. (The insertion-loss is, roughly speaking, the ratio of the transmitted power to the received power). For the usual application of the three-antenna method, three pairings of the antennas are used and the gains are obtained by algebraic solution from

the measured products G_1G_2, G_1G_3, and G_2G_3. If two of the antennas are identical and the gain of the third antenna is not needed it is easier and more accurate to determine the gains from the product G_1G_2 and ratio G_1/G_2. This ratio is measured by placing first one antenna and then the other with precisely the same orientations in a stable field generated with the third antenna; and the better accuracy occurs mainly cause some important sources of error, such as the proximity error, will be virtually the same for both antenna placements and also because the gain ratio will be very close to unity. The gain measurements reported here are based on this variation of the three-antenna method and thus involve both gain product and gain ratio measurements.

Antenna gain measurements of high accuracy are complex and involve many sources of uncertainty. A thorough analysis of these uncertainties and successful design and conduct of the measurements are greatly aided by developing appropriate "working" formulas, that is, equations derived specifically for the measurement at hand and relating directly to the particular techniques and equipment used. Though such formulas will likely be somewhat arbitrary in that they will reflect the personal style of the metrologist, the quality of the uncertainty analysis, and therefore the confidence that can be placed in the results, will be determined to a large extent by the working formulas since they embody the soundness, completeness, and logic of the overall measurement scheme. The two working formulas used in this report are discussed briefly below. The formula for the product of the gains is:

$$G_T G_R = \left(\frac{4\pi d}{\lambda}\right)^2 \left(\frac{i_{P_L}}{f_{P_{LO}}} \frac{f_{P_A}}{i_{P_A}}\right)^{-1} \left(\frac{NM}{DP}\right) \qquad (1)$$

G_T and G_R are the maximum values of the gain functions, respectively, the transmitting antenna and receiving antenna; d is the separation distance between the antennas, λ is the wavelength in the transmitting medium, $i_{P_{LO}}$ is the power dissipated by the load due to direct transmission from the transmitting antenna (that is, minus multipath interference or extraneous receptions from other sources); f_{P_L} is the power dissipated in the load when the generator and load are directly coupled; i_{P_A} is the available power from the generator during the antenna transmission; f_{P_A} is the power available from the generator during the direct coupling of the generator and load; and N, M, D, and P, defined below, are factors that express the effects of such things as misalignment of the antennas or waveguide mismatch that are usually considered to be deviations from the desired ideal situation.

In the sense that N, M, D, and P represent correctable deviations from ideal conditions, they are "correction factors" and will be so called in this report. N is a correction factor for finite separation between the antennas (the "proximity correction"), M is a waveguide mismatch factor, D is the product of the normalized directivities of the antennas, and P is a polarization mismatch factor. N and D do not have simple, exact expressions in terms of other parameters, but M and P can be expressed algebraically:

$$M \equiv \frac{|1 - \Gamma_G\Gamma_T|^2 \; |1 - \Gamma_R\Gamma_L|^2}{(1 - |\Gamma_T|^2)(1 - |\Gamma_R|^2) \; |1 - \Gamma_G\Gamma_L|^2} \qquad (2)$$

where Γ_G is the (waveguide) reflection coefficient of the generator, Γ_T is the reflection coefficient of the transmitting antenna when radiating into free space, Γ_R is the reflection coefficient of the receiving antenna when used as a radiator into free space, and Γ_L is the reflection coefficient of the load; and

$$P \equiv \frac{|1 - P_T P_R|^2}{(1 = |P_T|^2)(1 = |P_R|^2)} \qquad (3)$$

where P_T is the linear polarization index of the transmitting antennas and P_R is the linear polarization index of the receiving antenna when used for transmitting.

By using (1) twice, once for each transmission from a reference antenna to the two antennas being measured, it is easily shown that the ratio of the gains of the two antennas can be expressed by

$$\frac{G}{G'} = \frac{d}{d'}^2 \frac{P_{LO}}{P'_{LO}} \frac{P_A'}{P_A} \frac{\frac{N}{N'}\frac{M}{M'}}{\frac{D'}{D}\frac{P'}{P}} \qquad (4)$$

The uncertainty estimates are the simple sum of the individual error components listed in the following table. Each uncertainty component is estimated for worst case conditions.

Uncertainty in Gain Measurement

Sources of Uncertainty	Uncertainty dB
Gain Product Measurement	
A. Conditions assumed	± .005
1. Antenna reciprocity and stability (20°C ± 10°C) ± .003 dB	
2. Equipment idealization ± .002 dB	
3. Transmitting medium idealizations 0 dB	
4. Assumed single source 0 dB	
B. Distance and wavelength	± .001
1. Distance measurement ± .001 dB	
2. Wavelength determination 0 dB	
C. Insertion Loss Measurement	± .004
1. Generator power ratio ± .001 dB	
2. Load power ratio ± .003 dB	
D. Proximity Correction N	a) ± .013 b) ± .009
1. Drift in load power measuring system ± .006 dB	
2. Interpolation for frequency	
a) 2282.5, 2292.5, 2295.0: ± .004 dB	
b) 2277.5, 2287.5, 2297.5: 0 dB	
3. All other sources ± .003	
E. Mismatch factor M	± .002
F. Directivity misalignment	± .001
G. Polarization factor	± .001
Gain Ratio Measurement	
A. Condition assumed	± .003
1. Antenna reciprocity and stability ± .001 dB	
2. Equipment idealization ± .002 dB	
3. Transmitting medium idealization 0 dB	
4. Assumed single source 0 dB	
B. Distance and Wavelength	0
1. Distance stability 0 dB	
2. Wavelength stability 0 dB	

C.	Power ratio measurements	± .003
	1. Generator power ratio ± .001 dB	
	2. Load power ratio ± .002 dB	
D.	Ratios of correction factors	± .001
	1. Proximity corrections 0 dB	
	2. Mismatch factor 0 dB	
	3. Directivity factor 0 dB	
	4. Polarization factor ± .001 dB	
E.	Interpolation for frequency	a) ± .001
		b) 0
	a) 2282.5, 2292.5, and 2295.0 ± .001 dB	
	b) 2277.5, 2287.5, and 2297.5 0 dB	

Total uncertainties

a) 2282.5, 2292.5, and 2295.0	± .036
b) 2277.5, 2287.5, and 2297.5	± .031

Wavelength in air at 1600m elevation, 20°C and 40% relative humidity was used, which means that the gains determined are for operation of the antennas in air at this elevation. For vacuum, the gains of the antennas would be approximately 0.001 dB less.

(1) M. Kanda, "Considerations in the Measurement of Power Gain of a Large Microwave Antenna," IEEE Trans. Antennas and Propagation, pp. 407-411, May 1975.

(2) M. Kanda, "An Error Analysis for Absolute Flux Density Measurements of Cassiopeia A," IEEE Trans. on Instrumentation and Measurement, Vol. IM-25 No. 3, pp. 173-182, September 1976.

(3) A. C. Newell, R. C. Baird, and P. F. Wacker, "Accurate Measurement of Antenna Gain and Polarization at Reduced Distances by an Extrapolation Technique," IEEE Trans. Antennas and Propagation, Vol. AP-21, pp. 418-431, July 1973.

For the Director,
Institute for Basic Standards

C K S Miller by FAR

C. K. S. Miller, Chief
EMI/Radiation Hazards Metrology Program
Electromagnetics Division

APPENDIX B

OPERATING INSTRUCTIONS FOR LINEARITY MEASUREMENTS

C. T. Stelzried/M. S. Reid, 238-737, x-3332

OPERATING INSTRUCTIONS FOR

LINEARITY MEASUREMENTS (CTS22A)

DSS 11, 12, 13 and 14

Revision July 21, 1970

(1) Record station number.

(2) Record cone type, serial number and modification number.

(3) Record operator's initials.

(4) Record frequency in MHz.

(5) Record date and time (GMT).

(6) Record any suitable comments, such as problems experienced with the equipment or unusual conditions, etc.

(7) (i) Signal generator off.

(ii) Set the waveguide switch to the ambient load.

(iii) Adjust the IF attenuator to yield a suitable reference position and record the IF attenuator reading.

(8) (i) Set the waveguide switch to the antenna.

(ii) Adjust the IF attenuator for the same reference position found in 7(iii) above and record the IF attenuator reading.

(9) Turn the signal generator on.

(10) Set the IF attenuator approximately midway between the readings of (7) and (8).

etc. Adjust the signal generator attenuator for an even dB reading near the reference position and record the setting. Adjust the IF attenuator accurately to the reference position and record the setting. Decrease the signal generator settings in 2 dB steps and return to the reference position by adjusting the IF attenuator. Repeat until the form is complete.

LINEARITY MEASUREMENTS CTS/22A

JPL Computer Program 5925000

(1) Station: 1

(2) Cone: Type 3 SN 6 Mod 8

(3) Operator: 12

(4) Frequency (MHz): 15

(5) Time (GMT): Year 24 Day No. 26 Hour:Min. 29

(6) Comments: 33

CARD 1

Signal Generator Off

(7) Waveguide Switch on Ambient Load
Adjust IF Attenuator for Reference Position 1

(8) Waveguide Switch on Antenna
Adjust IF Attenuator for Reference Position 11

CARD 2

Signal Generator On, Waveguide Switch on Antenna

(9) IF, dB 1 6 11 16 21

(10) SG, dB 1 11 16 21

(11) IF, dB 26 31 36 41 46

(12) SG, dB 26 31 36 41 46

(13) IF, dB 51 56 61 66 71

(14) SG, dB 51 56 61 66 71

CARD 3

CARD 4

APPENDIX C

OPERATING INSTRUCTIONS FOR RADIO SOURCE NOISE TEMPERATURE CALIBRATION AND SAMPLE DATA

A. J. Freiley, 238-737, x-6418

OPERATING INSTRUCTIONS FOR RADIO SOURCE NOISE TEMPERATURE CALIBRATION (AJF/1)

Revision August 25, 1972

(1) Record station number.

(2) Record cone type, serial number, modification number, and the polarization configuration according to the code shown on the form.

(3) Record the maser serial number.

(4) Indicate receiver identification, such as DSN, monitor, or special configuration, etc. Each station should use one maser-receiver-detector configuration as the star-track standard, in order to avoid different configurations for long term system performance monitoring.

(5) Record IF attenuator serial number.

(6) Record operator's(s') initials.

(7) Record day number and year (GMT).

(8) Record outside weather conditions.

(9) Record comments on outside weather conditions such as overcast, clear night, windy, light rain, etc.

(10) Record the numeral 1 if the various conditions are true or zero if any one is not true.

(11) Identify the radio source.

(12) Record operating frequency.

(13) Record any suitable comments, such as problems experienced with the equipment or unusual conditions, or any further weather comments.

(14) Set the waveguide switch to ambient load. The signal generator must be on full attenuation. The maser is to be turned off and on with the magnet current. Leave in the off condition as short a time as possible. Set the power meter range switch to -15 dBm.

(i) Stations with a level set attenuator

Set one of the controls on the level set attenuator to the position Z_0. (This represents an infinite attenuation)

(a) Turn the maser off.

(b) Set the IF attenuator to 0.0 dB and record this setting. Observe the power level indicated on the power meter face.

(c) Take the level set attenuator off the Z_0 position. Adjust the level set attenuator to raise the reading on the power meter face by 1 dB.

(ii) Stations without a level set attenuator

(a) Turn the maser off.

(b) Increase the attenuation on the IF attenuator until the power level shown on the power meter face no longer decreases.

(c) Adjust the IF attenuator so that the power level indicated on the power meter face increases by 1 dB, then record the IF attenuator setting.

All stations

(d) Turn the maser on and peak the maser gain.

(e) Adjust the IF attenuator for the same power meter indication noted in (c) and record this IF attenuator reading.

(15) Waveguide switch on the ambient load. Set the signal generator on frequency. (Watch for frequency pulling.) Power meter range switch set on -15 dBm.

(a) Adjust IF attenuator for -2 dBm indication on power meter face.

(b) Set coaxial switches to Ref/Gain.

(c) Adjust signal generator attenuator for -1 dBm indication on power meter face, and record the signal generator attenuator setting.

(d) Set the coaxial switches on Maser/Gain.

(e) Repeat (c).

(16) Record ambient load temperature in degrees Centigrade.

(17) Record antenna boresight offsets (degrees). Unless otherwise noted, Declination and Hour Angle offsets are desired.

(18) Record time (GMT)

(19) Record antenna elevation angle (deg.)

(20) Record ambient load temperature (°C)

These should be recorded after attenuator reading Line (23) Item 31 while still on source.

(21) Record any difficulties and/or observations during this data block.

(22) IF attenuator Y-factors. The three conditions are: (i) antenna off
(23) source, (ii) antenna on source, (iii) waveguide switch on ambient load.
(24) A smooth procedure is important and should be developed with servo/microwave cooperation for rapid, precise off-on source antenna slewing coupled with smooth IF attenuator manipulation on the increasing noise powers being measured.

As one time saving move, it is recommended that item (24) positions 43 and 49 (typical), may be obtained while the servo is driving off source to prepare for item (22), positions 7 and 13 (typical). Most reliable Y-factors will be obtained when a time minimum is attained for item (22) to item (23) (typical). This puts the burden on good servo performance.

The table shown below is a (conservative) guide for off source angles.

Recommended Off Source Angles

Antenna	Frequency Band	Source Above 60° Elevation	Source Below 60° Elevation
26-m	S	±5° in elevation	±5° in azimuth
26-m	X	±1° in elevation	±1° in azimuth
64-m	S	±2° in elevation	±2° in azimuth
64-m	X	±1° in elevation	±1° in azimuth
64-m	K	±1° in elevation	±1° in azimuth

Note: At the operator's option, additional second pages of data sheets may be attached to the first page. The operator should consider the applicability of page 1 data as the breakpoint for initiating an up-dated page 1. For generally average conditions it is expected a single page 1 per 8 hour period is adequate.

RADIO SOURCE NOISE TEMPERATURE CALIBRATION AJF/1

JPL COMPUTER PROGRAM A083

(1) Station: (1)

(2) Feedcone: Type (4) Serial (8) Modif. (11)

Polarization (0,1,2 for RCP, LCP, Linear) (13)

(3) Maser: Serial (15)

(4) Receiver: (21)

(5) IF Attenuator: Serial (33)

(6) Operator: (39) (43)

(7) Date (GMT): Day No. (47) Year (50) Hour: Min. (52)

(1) (80)

---

(8) Outside Weather: Humidity (%) (1) Temperature (°C) (3)

(9) Weather Conditions: (7)

(10) Record 1 for YES: Clear Weather; Sun not in Beam; No RF Spur; No Water on Horn. (27)

(11) Radio Source: (28)

(12) Frequency (MHz): (41)

(13) Comments: (49) (2) (80)

---

(14) Maser OFF-ON (dB) on Ambient Load: OFF (1) ON (5)

(15) Maser Gain (dB) on Ambient Load: REF/GAIN (10) MASER/GAIN (15)

(16) Ambient Load Temperature (°C) (20) (3) (80)

Page ____ of ____

PAGE 1 JPL 1766 R 9/72

(17) Antenna Boresight Offsets (DEG): HA or AZ (1) DEC or EL (6)

(18) Time (GMT): Hour: Min (11)

(19) Antenna Elevation Angle (DEG): (15)

(20) Ambient Load Temp. (°C): (19)

Record after Attenuator Reading Line 23 Item 31 While still on Source

(21) Comments: (24–55), (56–77), (4, 80)

IF ATTENUATOR READINGS (dB)

(22) Antenna OFF Source: (1), (7), (13), (19)

(23) Antenna ON Source: (25), (31), (37)

(24) Ambient Load: (43), (49), (55), (5, 80)

(17) Antenna Boresight Offsets (DEG): HA or AZ (1) DEC or EL (6) (If reboresighted)

(18) Time (GMT): Hour: Min (11)

(19) Antenna Elevation Angle (DEG): (15)

(20) Ambient Load Temp. (°C): (19)

Record after Attenuator Reading Line 23 Item 31 While still on Source

(21) Comments: (24–55), (56–77), (4, 80)

IF ATTENUATOR READINGS (dB)

(22) Antenna OFF Source: (1), (7), (13), (19)

(23) Antenna ON Source: (25), (31), (37)

(24) Ambient Load: (43), (49), (55), (5, 80)

(17) Antenna Boresight Offsets (DEG): HA or AZ (1) DEC or EL (6) (If reboresighted)

(18) Time (GMT): Hour: Min (11)

(19) Antenna Elevation Angle (DEG): (15)

(20) Ambient Load Temp. (°C): (19)

Record after Attenuator Reading Line 23 Item 31 While still on Source

(21) Comments: (24–55), (56–77), (4, 80)

IF ATTENUATOR READINGS (dB)

(22) Antenna OFF Source: (1), (7), (13), (19)

(23) Antenna ON Source: (25), (31), (37)

(24) Ambient Load: (43), (44), (55), (5, 80)

Page ____ of ____

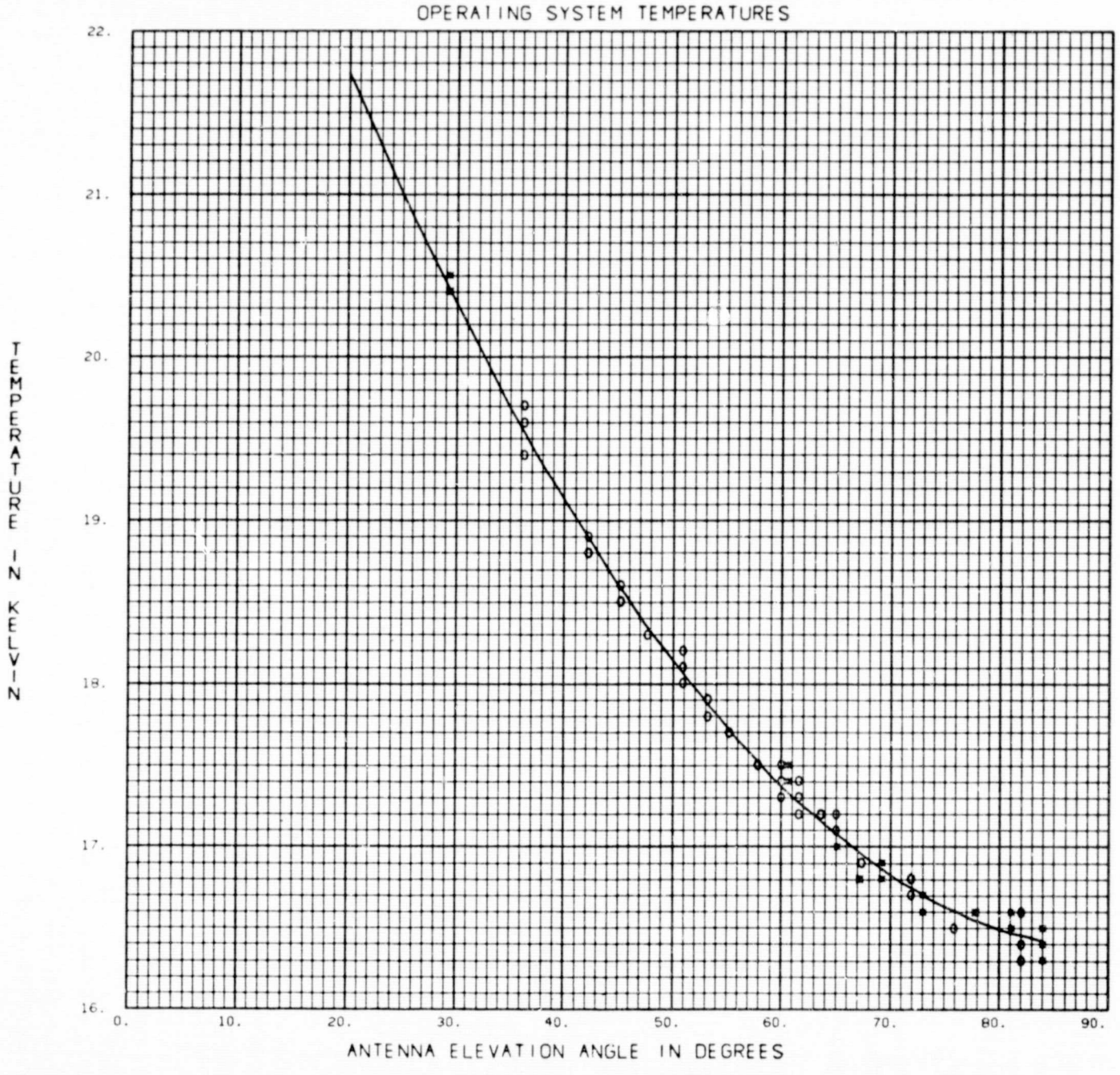

STA	YEAR	MONTH		RADIO SOURCE	FREQ,MHZ	RANGE	OP.TEMP,K	MAX	MIN	ST.DEV.	SO.TEMP,K	MAX	AT	ST.DEV
013	72	054	72	CYGNUS A	2278.50			21.7	18.4	.085				

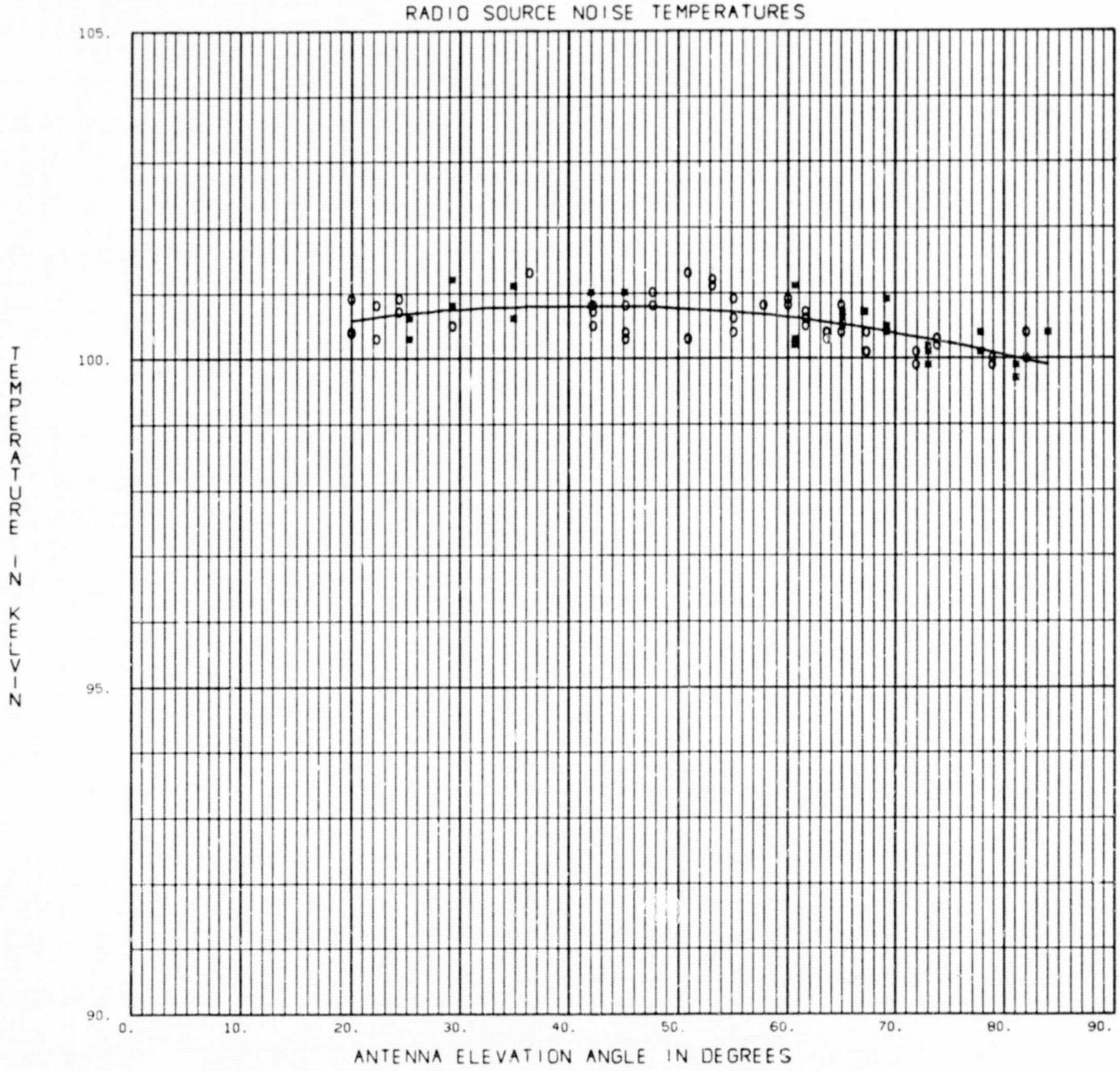

STA	YEAR	MONTH		RADIO SOURCE	FREQ,MHZ	RANGE	OP.TEMP,K	MAX	MIN	ST.DEV.	SO.TEMP,K	MAX AT	ST.DEV
013	72	054	72	CYGNUS A	2278.50			21.7	16.4	.085			

JPL Y,M100-8-41.0,DEG2,14278 ,1108

RADIO SOURCE NOISE TEMPERATURE CALIBRATION

STATION	013
FEEDCONE	TYPE SRO SERIAL NUMBER 001 MODIFICATION 00
	POLARIZATION 0 RCP
MASER	SERIAL NUMBER 9655
RECEIVER	MOD IV
I.F. ATTENUATOR	SERIAL NUMBER
OPERATOR	ECM
DATE (GMT)	DAY NUMBER 054 YEAR 72 HHMM 940

NO I.F. ATTENUATOR IDENTIFICATION SPECIFIED

OUTSIDE WEATHER	HUMIDITY 40 PER CENT	TEMPERATURE 9.0 (DEG C)
WEATHER CONDITIONS	CLEAR	
	CLEAR WEATHER	
	SUN NOT IN BEAM	
	NO R.F. SPUR	
	NO WATER ON HORN	ANSWER GIVEN: YES
RADIO SOURCE	CYGNUS A	
FREQUENCY (MHZ)	2278.5	
COMMENTS	SCOUR BORESIGHTING	

MASER OFF-ON (DB) OFF 10.4 ON 30.9
ON AMBIENT LOAD

MASER GAIN (DB) REF/GAIN 3.8 MASER/GAIN 16.0
ON AMBIENT LOAD

AMBIENT LOAD TEMPERATURE (DEG C) 25.60

MASER GAIN 45.20 DB FOLLOW ON TEMP. .271+01 K

END OF FILE ENCOUNTERED. PROCESS ONE DATA SET.

RADIO SOURCE NOISE TEMPERATURE CALIBRATION

ANTENNA BORSIGHT OFFSETS (DEG) DEC OR EL -.052 HA OR AZ .103 (IF REBORSIGHTED) BLOCK 1

TIME (GMT) HOUR:MIN 11:55

ANTENNA ELEVATION ANGLE (DEG) 25.4

AMBIENT LOAD TEMPERATURE (DEG C) 25.60

	Y-FACTOR ATTENUATOR READINGS (DB):				INITIAL		FINAL	
					AVERAGE	SIGMA	MEAN	SIGMA
ANTENNA OFF SOURCE	25.260	25.270	25.200	25.200				
ANTENNA ON SOURCE	32.800	32.780	32.770					
AMBIENT LOAD	36.780	36.800	36.770					
ANTENNA SYSTEM TEMP.	21.551*	21.305*	21.280*		21.378	.150	20.940	*******
SOURCE TEMP.	100.621	99.748*	100.331		100.233	.445	100.690	.365

COMMENTS

ANTENNA BORSIGHT OFFSETS (DEG) DEC OR EL -.020 HA OR AZ .093 (IF REBORSIGHTED) BLOCK 2

TIME (GMT) HOUR:MIN 12:17

ANTENNA ELEVATION ANGLE (DEG) 29.3

AMBIENT LOAD TEMPERATURE (DEG C) 24.86

	Y-FACTOR ATTENUATOR READINGS (DB):				INITIAL		FINAL	
					AVERAGE	SIGMA	MEAN	SIGMA
ANTENNA OFF SOURCE	25.130	25.120	25.130	25.130				
ANTENNA ON SOURCE	32.850	32.870	32.850					
AMBIENT LOAD	36.850	36.860	36.880					
ANTENNA SYSTEM TEMP.	20.484	20.437	20.367		20.429	.059	20.409	.064
SOURCE TEMP.	100.832	101.159	100.115*		100.701	.534	100.740	.430

COMMENTS